

SANDIA REPORT

SAND98-0878

Unlimited Release

Printed September 1998

Interpretation of Data Obtained from Non-Destructive and Destructive Post-Test Analyses of an Intact-Core Column of Culebra Dolomite

W. George Perkins, Daniel A. Lucero

Prepared by
Sandia National Laboratories
Albuquerque, New Mexico 87185 and Livermore, California 94550

Sandia is a multiprogram laboratory operated by Sandia Corporation, a Lockheed Martin Company, for the United States Department of Energy under Contract DE-AC04-94AL85000.

Approved for public release; further dissemination unlimited.



Sandia National Laboratories

SAND98-0878
Unlimited Release
September 1998

Interpretation of Data Obtained from Non-Destructive and Destructive Post-Test Analyses of an Intact-Core Column of Culebra Dolomite

W. George Perkins
WIPP Regulatory Compliance Department

Daniel A. Lucero
WIPP Chemical and Disposal Room Processes Department

Sandia National Laboratories
P. O. Box 5800
Albuquerque, NM 87185-1395

ABSTRACT

The U.S. Department of Energy (DOE) has been developing a nuclear waste disposal facility, the Waste Isolation Pilot Plant (WIPP), located approximately 42 km east of Carlsbad, New Mexico. The WIPP is designed to demonstrate the safe disposal of transuranic wastes produced by the defense nuclear-weapons program. Performance assessment analyses (U.S. DOE, 1996) indicate that human intrusion by inadvertent and intermittent drilling for resources provide the only credible mechanisms for significant releases of radionuclides from the disposal system. These releases may occur by five mechanisms: (1) cuttings, (2) cavings, (3) spallings, (4) direct brine releases, and (5) long-term brine releases. The first four mechanisms could result in immediate release of contaminant to the accessible environment. For the last mechanism, migration pathways through the permeable layers of rock above the Salado are important, and major emphasis is placed on the Culebra Member of the Rustler Formation because this is the most transmissive geologic layer in the disposal system. For reasons of initial quantity, half-

Issued by Sandia National Laboratories, operated for the United States Department of Energy by Sandia Corporation.

NOTICE: This report was prepared as an account of work sponsored by an agency of the United States Government. Neither the United States Government nor any agency thereof, nor any of their employees, nor any of their contractors, subcontractors, or their employees, makes any warranty, express or implied, or assumes any legal liability or responsibility for the accuracy, completeness, or usefulness of any information, apparatus, product, or process disclosed, or represents that its use would not infringe privately owned rights. Reference herein to any specific commercial product, process, or service by trade name, trademark, manufacturer, or otherwise, does not necessarily constitute or imply its endorsement, recommendation, or favoring by the United States Government, any agency thereof, or any of their contractors or subcontractors. The views and opinions expressed herein do not necessarily state or reflect those of the United States Government, any agency thereof, or any of their contractors.

Printed in the United States of America. This report has been reproduced directly from the best available copy.

Available to DOE and DOE contractors from
Office of Scientific and Technical Information
P.O. Box 62
Oak Ridge, TN 37831

Prices available from (615) 576-8401, FTS 626-8401

Available to the public from
National Technical Information Service
U.S. Department of Commerce
5285 Port Royal Rd
Springfield, VA 22161

NTIS price codes
Printed copy: A06
Microfiche copy: A01



life, and specific radioactivity, certain isotopes of Th, U, Am, and Pu would dominate calculated releases from the WIPP. In order to help quantify parameters for the calculated releases, radionuclide transport experiments have been carried out using five intact-core columns obtained from the Culebra dolomite member of the Rustler Formation within the Waste Isolation Pilot Plant (WIPP) site in southeastern New Mexico. This report deals primarily with results of analyses for ^{241}Pu and ^{241}Am distributions developed during transport experiments in one of these cores. All intact-core column transport experiments were done using Culebra-simulant brine relevant to the core recovery location (the WIPP air-intake shaft - AIS). Hydraulic characteristics (i.e., apparent porosity and apparent dispersion coefficient) for intact-core columns were obtained via experiments using conservative tracer ^{22}Na . Elution experiments carried out over periods of a few days with tracers ^{232}U and ^{239}Np indicated that these tracers were weakly retarded as indicated by delayed elution of these species. Elution experiments with tracers ^{241}Pu and ^{241}Am were performed, but no elution of either species was observed in any flow experiment to date, including experiments of many months' duration. In order to quantify retardation of the non-eluted species ^{241}Pu and ^{241}Am after a period of brine flow, non-destructive and destructive analyses of an intact-core column were carried out to determine distribution of these actinides in the rock. Analytical results indicate that the majority of the ^{241}Am is present very near the top (injection) surface of the core (possibly as a precipitate), and that the majority of the ^{241}Pu is dispersed with a very high apparent retardation value. The ^{241}Pu distribution is interpreted using a single-porosity advection-dispersion model, and an approximate retardation value is reported for this actinide. The specific radionuclide isotopes used in these experiments were chosen to facilitate analysis. Even though these isotopes are not necessarily the same as those that are most important to WIPP performance, they are isotopes of the same elements, and their chemical and transport properties are therefore identical to those of isotopes in the inventory.

Table of Contents

INTRODUCTION.....	1
CORE SELECTION AND EXPERIMENTAL SUMMARY.....	3
FLOW EXPERIMENTS AND NON-DESTRUCTIVE ANALYSES	5
Flow and Injection Conditions	5
Autoradiography.....	5
Surface γ -Ray Spectrometry.....	7
DESTRUCTIVE POST-TEST ANALYSES	11
Sampling and Analysis Equipment and Techniques	11
Destructive Analysis Results.....	14
INTERPRETATION OF ANALYSIS RESULTS	17
Actinide Concentration Profiles	17
Estimation of Retardation Parameters.....	21
DISCUSSION	25
CONCLUSIONS.....	27
REFERENCES.....	29
APPENDIX A MICROSOFT EXCEL SPREADSHEET OF RAW LIQUID SCINTILLATION COUNTING DATA	A-1
APPENDIX B MICROSOFT EXCEL SPREADSHEET USED TO CALCULATE ACTINIDE CONCENTRATION VS. DEPTH RESULTS OF CALCULATION.....	B-1
APPENDIX C MICROSOFT EXCEL SPREADSHEET USED TO CALCULATE ACTINIDE CONCENTRATION VS. DEPTH FORMULAS.....	C-1
APPENDIX D DIMENSIONLESS FORM OF LINEAR-EQUILIBRIUM TRANSPORT EQUATION FOR E-CORE EXPERIMENTS	D-1
APPENDIX E DERIVATION OF RELATION BETWEEN DISSOLVED ACTINIDE CONCENTRATION AND TOTAL ACTINIDE CONCENTRATION IN THE ROCK.....	E-1
APPENDIX F LISTINGS OF POSITION-TIME INPUT FILES (*.INP) FOR COLUMN 1.4 CALCULATIONS	F-1
APPENDIX G LISTINGS OF PARAMETER INPUT FILES (*.COL) FOR COLUMN 1.4 CALCULATIONS	G-1
APPENDIX H LISTINGS OF OUTPUT FILES (*.LOG) FOR COLUMN 1.4 CALCULATIONS	H-1

APPENDIX I	LISTINGS OF EXCEL 97 SPREADSHEETS SHOWING CALCULATED VS. OBSERVED ACTINIDE CONCENTRATION AS FUNCTION OF DEPTH.....	I-1
APPENDIX J	MEMORANDUM FROM LOS ALAMOS NATIONAL LABORATORY CHEMICAL SCIENCE AND TECHNOLOGY DIVISION	J-1

TABLES

Table 1. Borehole properties.....	3
Table 2. Test sample core properties.....	3
Table 3. Summary of E-Core flow experiments.....	5
Table 4. Post-Test Evaluation Equipment.....	14
Table 5. Raw Results of Destructive Analysis of E-Core	15
Table 6. Approximate Actinide Activity per Unit Volume as Function of Depth	18

FIGURES

Figure 1. Autoradiographic image of the injection surface of E-Core using a 96-hour exposure of x-ray film to 59.5 keV ^{241}Am γ -rays.....	6
Figure 2. Relative distribution of γ -emitting radionuclide ^{241}Am on E-Core top surface.....	8
Figure 3. Schematic diagram of experimental set up used to scan longitudinal distribution of the γ -emitting radionuclide ^{241}Am in E-Core.....	9
Figure 4. Relative distribution with depth from top surface of γ -emitting radionuclide ^{241}Am in E-Core. Data are given for four angular positions around the circumference.....	9
Figure 5a. Photographs of the test apparatus used for milling the top surface of E-Core. (a) Drill press and vise on X-Y table.	12
Figure 5b. Photographs of the test apparatus used for milling the top surface of E-Core. (b) Pyrex glass cover plate, vacuum sample-collection hose, and in-line Nuclepore filter.....	13
Figure 6a. Measured ^{241}Am activity per unit rock volume as a function of depth.....	19
Figure 6b. Measured ^{241}Pu activity per unit rock volume as a function of depth.	19
Figure 7. Comparison of measured ^{241}Am activity per unit rock volume to results of calculation for retardation factor $R = 160,000$	23
Figure 8. Comparison of measured ^{241}Am activity per unit rock volume to results of calculation for retardation factor $R = 1,000,000$	23
Figure 9. Comparison of measured ^{241}Pu activity per unit rock volume to results of calculation for retardation factor $R = 160,000$	24
Figure 10. Comparison of measured ^{241}Pu activity per unit rock volume to results of calculation for retardation factor $R = 1,000,000$	24

INTRODUCTION

Under the authorization of Public Law 96-164 (1979), the U.S. Department of Energy (DOE) has been developing a nuclear waste disposal facility, the Waste Isolation Pilot Plant (WIPP), located approximately 42 km east of Carlsbad, New Mexico. The WIPP is designed to demonstrate the safe disposal of transuranic wastes produced by the defense nuclear-weapons program. Transuranic waste is defined as waste contaminated with radionuclides having an atomic number greater than 92, a half-life greater than 20 years and a concentration greater than 100 nCi/g (U.S. EPA, 1993). This radioactive waste is regulated by U.S. Environmental Protection Agency regulations 40 CFR Part 191 (U.S. EPA, 1993). The regulation sets limits on cumulative radioactive release to the accessible environment over 10,000 years and requires that Performance Assessment (PA) analyses be performed to demonstrate WIPP facility compliance with the regulations.

PA analyses (U.S. DOE, 1996) indicate that human intrusion by inadvertent and intermittent drilling for resources provide the only credible mechanisms for significant releases of radionuclides from the disposal system. These releases may occur by five mechanisms: (1) cuttings, (2) cavings, (3) spallings, (4) direct brine releases, and (5) long-term brine releases. The first four mechanisms could result in immediate release of contaminant to the accessible environment. For the last mechanism, migration pathways through the permeable layers of rock above the Salado are important, and major emphasis is placed on the Culebra Member of the Rustler Formation because this is by far the most transmissive geologic layer in the disposal system. Considerable empirical and conceptual modeling work has been done on the hydrology (Meigs *et al.*, 1997) and contaminant-transport (Brush, 1998; Holt, 1997) characteristics of the Culebra dolomite.

The rationale for selection of certain isotopes of Th, U, Am, and Pu for Culebra transport calculations in PA is given in the WIPP Compliance Certification Application (CCA - U.S. DOE, 1996, Appendix WCA). For reasons of initial quantity, half-life, and specific radioactivity, the isotopes listed in the CCA would dominate calculated releases from the WIPP. The rationale for the specific isotopes used in the intact-core column experiments has to do with radiolytic analysis of the species and is discussed in detail by Lucero *et al.* (1998).

Empirical batch sorption experiments have provided most of the actinide-dolomite sorption values submitted for PA calculations (Brush, 1998). However, flow experiments with intact rock columns of Culebra dolomite have also been used to demonstrate actinide retardation. The intact-core column flow experiments provide information on the effects of advective fluid flow on sorption behavior in the Culebra dolomite at small scale. The technical scope and requirements for these experiments are described in a test plan (Lucero *et al.*, 1995) and in a report on the work (Lucero *et al.*, 1998). In the experiments, steady state flows of Culebra-relevant brine were first established in several intact-core columns that had been recovered from the Culebra at the location of the WIPP Air-Intake Shaft. At various times after steady-state flow was established in a given core, relatively small pulses of brine containing one or more dissolved radioactive species were injected into the general flow at the upstream end of the column. The effluent brine was then analyzed as a function of time by either γ -ray spectroscopy or liquid scintillation counting for each of the injected

species.

Experimental results indicate that species ^3H (as tritiated water) and $^{22}\text{Na}^+$ are “conservative tracers” that are not significantly retarded by surface-chemical interactions with the rock. As described by Lucero *et al.* (1998), elution times for ^3H and $^{22}\text{Na}^+$ were used to estimate core hydraulic characteristics such as apparent porosity and apparent dispersion coefficient. The actinide species $^{232}\text{UO}_2^{++}$ and $^{239}\text{NpO}_2^+$ have been observed to elute with some degree of retardation from all columns into which they were introduced. On the other hand, none of the isotopes ^{241}Am , ^{241}Pu , and ^{228}Th has been observed to elute from any of the columns into which they were introduced. The purpose of the analyses reported here is to characterize the transport of ^{241}Am and ^{241}Pu in one of the cores.

Transport retardation characteristics of the eluted radioactive species were inferred from species elution time dependence using computer code COLUMN (Budge, 1996; Brown *et al.*, 1997), a one-dimensional transport code, with single-porosity and dual-porosity capabilities, which has been approved for use under quality assurance procedures relevant to the WIPP Project (Sandia National Laboratories, 1996-1997). COLUMN 1.4 has been used to infer retardation parameters from radionuclide elution data for a large number of experiments (Lucero *et al.*, 1998).

Recent multirate modeling of field conservative tracer tests at the WIPP site (Meigs *et al.*, 1997), combined with consideration of the effects of scale (Holt, 1997), indicate that the single-porosity treatment of the small-scale intact rock-column elution experiments will tend to provide low values for retardation factors calculated for the eluted species.

For the non-eluted actinides, transport modeling could, at best, be used to estimate minimum retardation factors for these species, as has been done by Lucero *et al.*, (1998) using the single-porosity option of COLUMN 1.4. In a meeting among DOE/Sandia, the State of New Mexico, and the Environmental Evaluation Group (11 October 1996), it was decided that Sandia would perform non-destructive and destructive analyses of one or more of the cores into which non-eluting actinides had been introduced. The plan was confirmed in a meeting between DOE/Sandia and the National Academy of Sciences (11 February 1997). This report describes results and interpretation of the non-destructive and destructive analyses of a selected intact-core column. All experimental work was done in accordance with a test plan addendum prepared by Behl and Lucero (1996) and with an analysis plan prepared by Perkins (1998).

CORE SELECTION AND EXPERIMENTAL SUMMARY

After evaluation of the test conditions for retardation experiments performed with five intact-core columns, it was determined that intact-core column E, VPX27-7 (hereafter called E-Core), was an excellent candidate for post-test analysis, for the following reasons. In three flow tests performed on E-Core, ^{22}Na , ^{232}U , ^{239}Np , ^{241}Pu , and ^{241}Am were injected into the core at various times, but ^{228}Th was never injected. This isotope of thorium produces daughter products that could complicate the analysis for ^{241}Pu . The isotopes ^{22}Na , ^{232}U , ^{239}Np did, in fact, elute, and their transport characteristics were analyzed as reported by Lucero *et al.*, (1998).

Table 1 gives a description of the VPX27 borehole from which E-Core was recovered, and Table 2 summarizes the physical dimensions and estimated properties of E-Core. The porosity estimate given in Table 2 was calculated by Lucero *et al.*, (1998) and represents the estimated total porosity available in E-Core.

Table 1. Borehole properties

Borehole	VPX 27
Depth below surface (m)	219.8
Side of AIS	North
Borehole flow (L/min)	3.0
pH	8.10
Temperature (°C)	21.1

Table 2. Test sample core properties

Series	E
Core: VPX	27-7A
Cut core measurements	
Length (cm)	10.2
Diameter (cm)	14.5
Volume (cm ³)	1666
Wet weight (gm)	4102
Injection well diameter (cm)	6.35
Injection well depth (cm)	0.43
Estimated core properties	
Dry bulk density (g/cm ³)	2.38
Porosity	0.15

As stated earlier, the objective of the post-test analyses was to characterize the distributions of non-eluted radionuclides (^{241}Pu and ^{241}Am) in the core. Three techniques were used to evaluate the non-eluted radionuclides. Two techniques were non-destructive and the third was destructive. The first technique involved placing x-ray films in direct contact with the injection (top) end of the core. After exposure to the ^{241}Am 59.5-keV γ -rays and development, the film provided a low-resolution image of the top-surface ^{241}Am distribution. The second technique involved taking radial and longitudinal γ -ray scans using a low-energy germanium detector, then plotting the results to obtain qualitative, low-

resolution, top-surface and longitudinal distributions of the ^{241}Am 59.5-keV γ energy. The third technique involved mounting the core on a drill press equipped with an X-Y milling table, after which the top surface of the core was milled, the core material was collected, and quantitative analyses were performed for both ^{241}Pu and ^{241}Am .

FLOW EXPERIMENTS AND NON-DESTRUCTIVE ANALYSES

Detailed information on test materials, equipment, and procedures are presented in Lucero *et al.*, (1998) and WIPP Laboratory Notebooks (Lucero, 1995-1997). The sections below summarize the procedures used and parameters specific to E-Core analyses.

Flow and Injection Conditions

Table 3 summarizes test information for the flow experiments performed on E-Core, all of which were carried out using AIS brine. As indicated in Table 3, brine flow was begun December 20, 1995 (at the rate of 0.1 mL/min), paused on April 9, 1996, restarted on June 4, 1996 (at the reduced rate of 0.05 mL/min), and terminated on July 15, 1996. Also given in Table 3 are test flow times and analytical methods for eluted radioactive species. The time from first injection of ^{241}Pu and ^{241}Am to the second injection of ^{241}Am was 65 days, and the time from second injection of ^{241}Am to the pause in flow was 18 days. Finally, the time from restart (at 0.05 mL/min, half the original flow rate) to end of flow was 41 days (see Lucero *et al.*, 1998).

Table 3. Summary of E-Core flow experiments

Test Number	Tracer	Injection Mode	Pump Speed (mL/min)	Test Duration	Information from Test	Analytical Method(s)
E-1 (12/20/95)	3.2 $\mu\text{Ci } ^{22}\text{Na}$ 31 $\mu\text{Ci } ^{232}\text{U}$ 464 $\mu\text{Ci } ^{239}\text{Np}$	20 mL Spike	0.1	26 days	Physical & Chemical Retardation (U, Np)	γ -Ray Spectrometry for Na & Np α -Spectrometry or LSC for U
E-2 (1/16/96)	2.6 $\mu\text{Ci } ^{22}\text{Na}$ 11.3 $\mu\text{Ci } ^{241}\text{Pu}$ 12.2 $\mu\text{Ci } ^{241}\text{Am}$	18.5 mL Spike	0.1	65 days	Physical & Chemical Retardation (Am, Pu)	γ -Ray Spectrometry for Na & Am LSC for Pu
E-3 Live Microbes (3/22/96)	16 $\mu\text{Ci } ^{22}\text{Na}$ 136 $\mu\text{Ci } ^{232}\text{U}$ 13.4 $\mu\text{Ci } ^{241}\text{Am}$	20mL Am Spike 4 liters (Na, U, & microbes)	0.1	18 days	Microbe Effects on Physical & Chemical Retardation (U, Am)	γ -Ray Spectrometry for Na & Am LSC for U & Pu
Pause (4/9/96)						
Restart (6/4/96)			0.05	41 days		
End (7/15/96)						Start Post-Test Analyses

Autoradiography

E-Core was removed from its aluminum pressure vessel (for details about the pressure vessel and brine-pumping apparatus, see Lucero *et al.*, 1998). After removing the brine-distribution cap from the injection side of the core, x-ray films were placed on the exposed core surface for times up to 96 hours. The films were then processed at the Sandia National Laboratories non-destructive test facility. The developed films provided

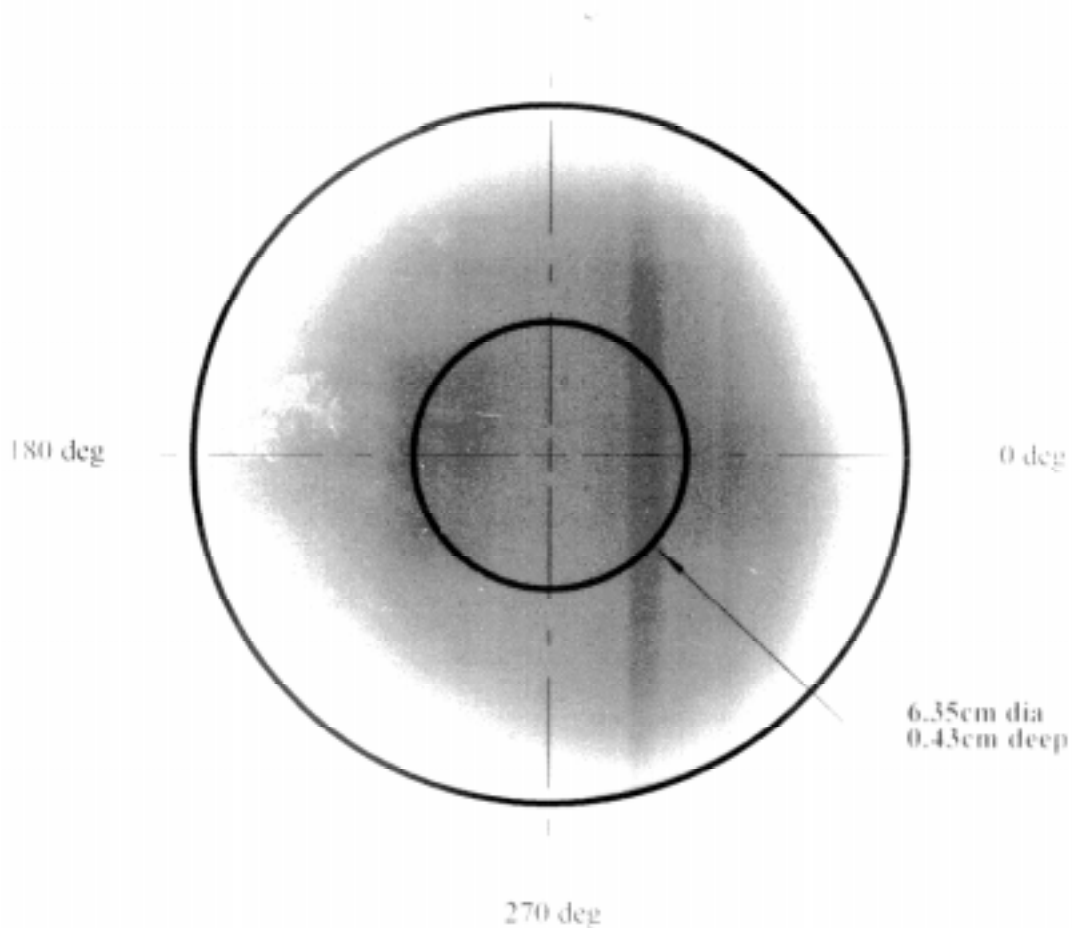


Figure 1. Autoradiographic image of the injection surface of E-Core using a 96-hour exposure of x-ray film to 59.5 keV ^{241}Am γ -rays.

qualitative information about the surface distribution of the injected ^{241}Am . In the low-resolution radiographic image shown in Figure 1 (96-hour exposure), the outside circumference of E-Core and the circumference of the brine-injection well are depicted as solid concentric circles. The film darkening then indicates the approximate distribution of ^{241}Am in and around the top-surface brine-injection well. Angular locations marked on the film are not easily readable. For reference, the right-hand limb of the circle is designated 0°, the top is 90°, the left-hand is 180°, and the bottom is 270°. The angular-location labels correspond to the location labels in subsequent figures.

Examination of the radiographic image of Figure 1 suggests that at least some of the ^{241}Am may have migrated outside the brine injection well. However, it is impossible to estimate this migration quantitatively based on the radiographic analyses. The method of autoradiography has at best very low resolution, perhaps of the order of several cm.

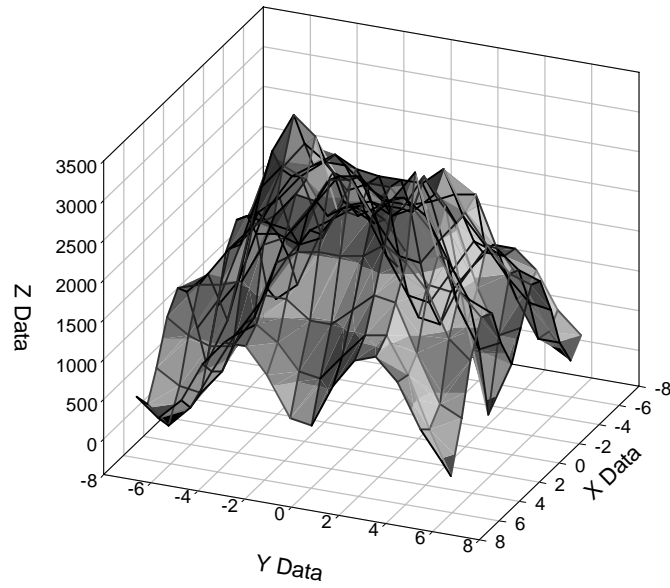
Surface γ -Ray Spectrometry

No straightforward non-destructive method was found to determine the distribution of ^{241}Pu , which emits a low-energy (20.8 keV) β .

Surface spectrometry could, however, be used for the γ -emitting radioisotope ^{241}Am . To map the ^{241}Am top-surface distribution, the core was placed horizontally on a vise mounted on an X-Y motion table, with the top surface facing a Ge γ -ray detector. The γ -ray counts at various locations on the injection surface of the core were measured by moving the core on the X-Y table. The resolution, precision, and accuracy for γ -ray counting were limited by the nonadjustable detector collimator aperture (5-mm diameter). The relative distribution of the γ -ray-emitting radionuclide ^{241}Am on the core surface, as shown in Figure 2, indicates that the majority of the ^{241}Am is localized within the brine-injection well, with some apparent signal detected outside the well. Since the resolution is at best 5 mm, it is not possible to determine quantitatively from either Figure 1 or Figure 2 how much ^{241}Am might actually reside outside the well boundary.

Surface spectrometry was also used to determine a qualitative longitudinal distribution of ^{241}Am , using the experimental set up shown schematically in Figure 3. For this measurement, the Ge γ -ray detector was fitted with a 5-mm diameter collimator and scanned vertically at 5-mm intervals from a point 5 mm above the top core surface to about 3 cm below the top surface. Scans were made at angular locations 0° , 90° , 180° , and 270° around the core circumference, as is indicated in Figure 3. Results of the scans are summarized in Figure 4, which shows no evidence for penetration of ^{241}Am beyond a depth of about 1 cm below the bottom of the injection well. Moreover, the apparent γ -ray signal above the core top surface reemphasizes that the fairly large aperture of the collimator on the γ -ray detector limits the spatial resolution to about 1 centimeter. The variation with angular position is probably real. However, it was not possible to correlate this variation with any apparent core features (e.g., with visible fractures).

Reasonably successful attempts were made to fit the qualitative low-resolution distribution data of Figure 4 using the COLUMN one-dimensional flow and transport code (Budge, 1996; Brown *et al.*, 1997) in its single-porosity mode to obtain a retardation parameter estimate consistent with the data shown in Figure 4. However, these results were clouded by the low resolution of the γ -ray scan data. As is shown in the discussion of the destructive analysis below, the actual ^{241}Am distribution is much narrower than is indicated by Figure 4.



E-Core 59keV γ -Ray Results

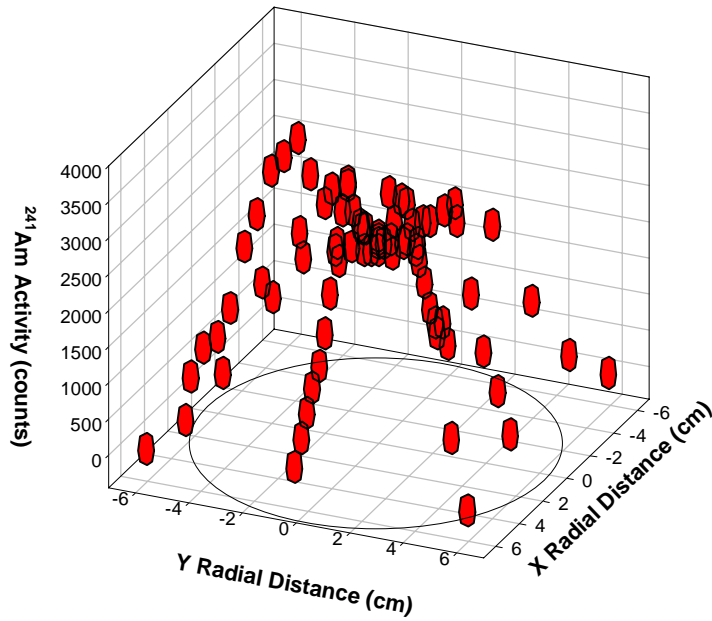


Figure 2. Relative distribution of γ -emitting radionuclide ^{241}Am on E-Core top surface.

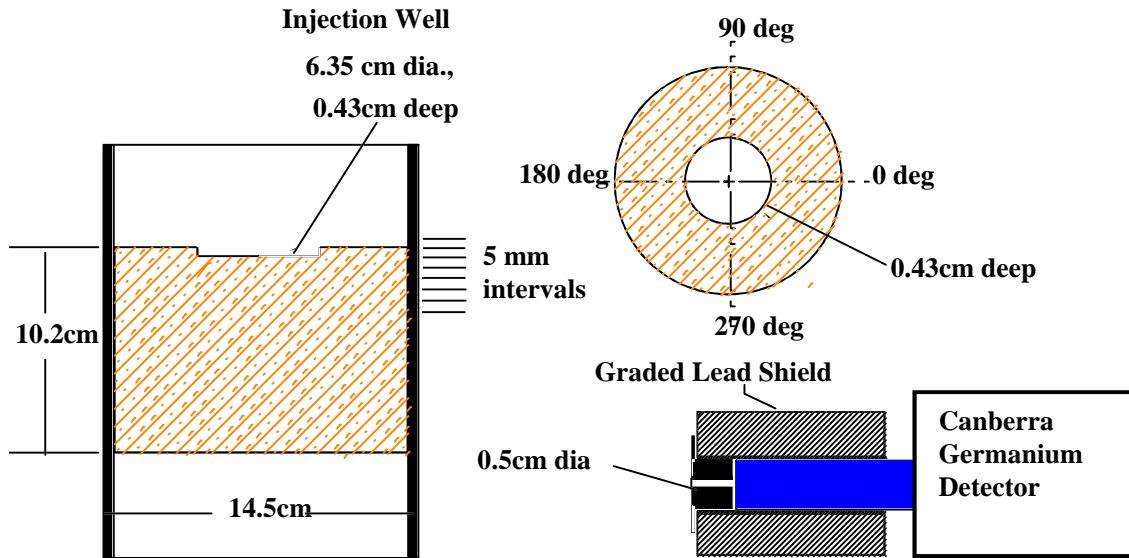


Figure 3. Schematic diagram of experimental set up used to scan longitudinal distribution of the γ -emitting radionuclide ^{241}Am in E-Core.

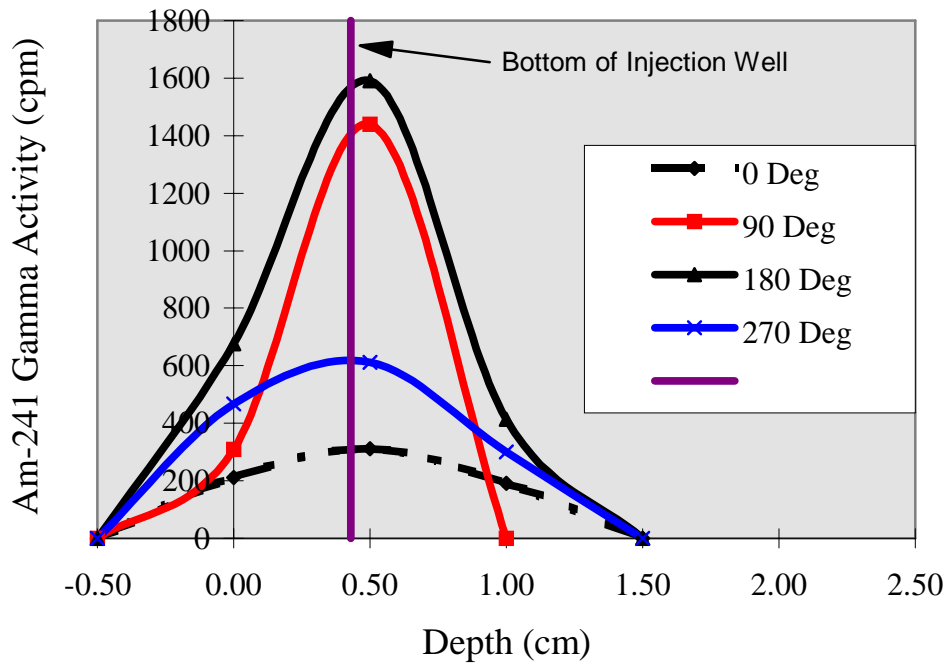


Figure 4. Relative distribution with depth from top surface of γ -emitting radionuclide ^{241}Am in E-Core. Data are given for four angular positions around the circumference.

DESTRUCTIVE POST-TEST ANALYSES

Prior information on the very strong adsorption of $^{241}\text{Am}^{3+}$ to dolomite, as well as the low-spatial-resolution γ -ray counting on E-Core, indicated that this species might have been transported only a short distance into the rock during elution experiments. Thus, it was decided to use a method in which very small amounts of rock would be removed sequentially from the brine injection region of E-Core and analyzed by appropriate radioactive counting techniques (Behl and Lucero, 1996). The experiments were carried out at the Sandia Tomography and Radioactive Transport (START) Laboratory.

Since the information gained from the non-destructive evaluation indicated that most of the γ -ray emitting radionuclide (^{241}Am) was distributed within the first 1 cm depth of the core, initial destructive analysis was planned for the top centimeter just below the fluid injection well with which E-Core is equipped.

Sampling and Analysis Equipment and Techniques

For radiation safety, the destructive sampling apparatus had to fit into and be operated inside a glove box, which limited the experimental options and required keeping the operation as simple as possible. Photographs of the apparatus are shown in Figure 5, and its more important components are listed in Table 4. Equipment used for the destructive analysis consisted of a Delta 12-inch bench drill press with a 0.25-inch diameter end mill. The core was secured in a Dayton 8-inch cross vise bolted to the drill-press table. Horizontal positioning (X and Y) was provided by the cross vise. A depth stop with scale calibrated in millimeters provided approximate vertical axis control (however, accurate depth of cut was inferred from recovered rock mass). The shank of the mill bit projected through a 0.375"-diameter hole in 6" \times 6" \times 0.25" pane of Pyrex glass which was positioned near the core top surface to minimize loss of powder. A vacuum hose with an in-line Nuclepore filter was positioned at the hole perimeter to capture rock powder on tare-weighed filter papers during the milling process.

Sample recovery and radiolytic analyses were performed in several steps:

- the solution-injection distribution plates (described in Lucero *et al.*, 1998) were acid washed with 0.1 N HCl to recover any actinide that might have sorbed on the equipment rather than on the rock;
- beginning on the floor of the solution-injection well (see Lucero *et al.*, 1998), the core was milled at 450 rpm until a preset depth stop was reached (initial milling cuts were done within the cylinder defined by the solution-injection well—later cuts expanded the diameter of the well in order to determine whether the actinides had diffused laterally);
- after the total area had been milled as controlled by a given depth stop, all of the core material from the cut was collected on the in-line filter via the vacuum hose or by physically picking up any macroscopic chunks;
- the rock powder and filter paper were re-weighed, the net powder mass was determined by subtracting the tare mass;



Figure 5a. Photographs of the test apparatus used for milling the top surface of E-Core; Drill press and vise on X-Y table.

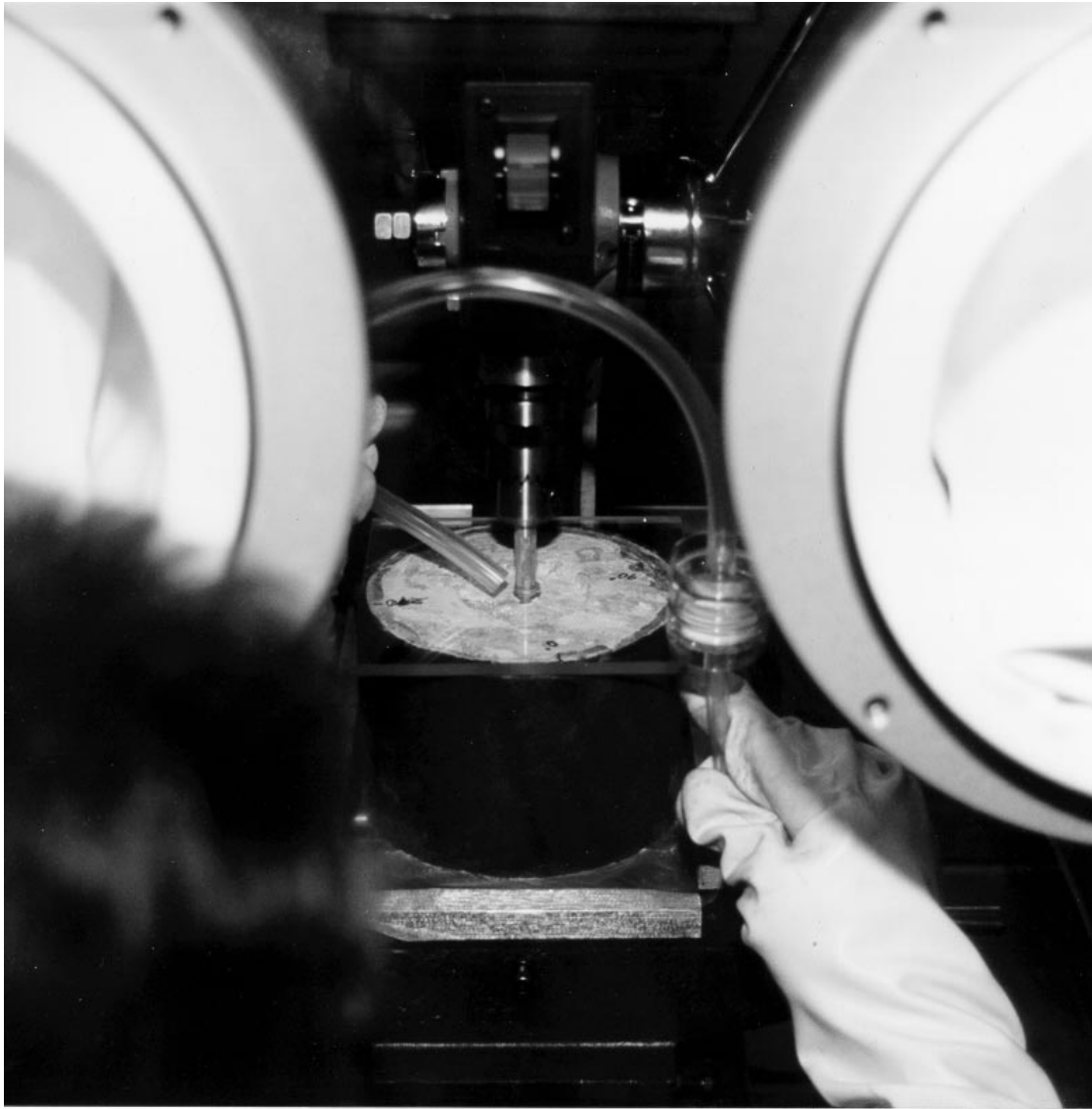


Figure 5b. Photographs of the test apparatus used for milling the top surface of E-Core; Pyrex glass cover plate, vacuum sample-collection hose, and in-line Nuclepore filter.

Table 4. Post-Test Evaluation Equipment

Equipment	Make	Model
12" Bench Top Drill Press	Delta	11-990
8" X-Y Cross Vise	Dayton	3W766
PM Balance	Mettler	PM1200
37-mm Particle Sampler	Gelman	4339
Vacuum Pump	Welch	8915
Automatic Gamma Spectrometer	Canberra	96-4980
Liquid Scintillation Counter	Packard	2550TR/AB
Portable Gamma Detector	Canberra	GL2020R
Portable Detector Shield	Canberra	717

- the rock powder and filter paper were transferred to a beaker containing 75 to 150 mL of 0.1N HCl;
- the acid solution was extracted with a syringe and injected into a number (several tens) of test tubes;
- the activity in each test tube was analyzed by γ -ray spectroscopy and/or liquid scintillation counting (LSC);
- using a Pentium Pro processor running under Windows NT 4.0, the activity in each test tube was recorded in a Microsoft Excel (v. 7.0a) spreadsheet and the total activity in a given cut was calculated by summing the test-tube activities using the Excel SUM function. The activity data spreadsheet is attached as Appendix A.

Test-tube contents were initially analyzed by γ -ray spectrometry for the γ -emitting ^{241}Am and liquid scintillation counting (LSC) for the β -emitting ^{241}Pu . However, it was discovered that fine powder suspended in the test tubes affected the γ -ray counting geometry adversely. Thus, the results reported here were obtained using LSC for both ^{241}Am (α) and ^{241}Pu (β). The total rock mass and total activity could then be used to determine the amount and concentration of actinide in each rock layer removed. In the Excel spreadsheet attached as Appendix A, column headings labeled "0.2 cm," "0.4 cm," etc. indicate the approximate depth of cut. Actual depth of cut was calculated from recovered mass and estimated density. Columns headed "mass" contain the total masses of test tubes and injected rock solutions (0.1 N HCl). Columns headed " $\mu\text{Ci}/\text{vial}$ " indicate LSC readings for the various vials containing dissolved actinide.

Destructive Analysis Results

As recorded in Table 2, the brine-injection well in E-Core was 6.35 cm diameter and 0.43 cm deep (Lucero *et al.*, 1998). The first two vertical milling cuts were performed beginning at the floor of this initial well. A horizontal circumferential cut was then made (at the new well depth) to determine whether there had been significant lateral actinide migration into the wall of the well. Six additional vertical cuts were then made to increase the well depth at the new diameter, 7.2 cm. Finally, a circumferential cut was made that added 0.8 cm to the well diameter to a depth of approximately 0.5 cm. The total mass of recovered rock was recorded at the end of each cut. The depth of each cut was calculated from the recovered rock mass, the estimated rock density (see Table 2), and the well

diameter, which was assumed to remain approximately circular throughout the experiment. Total rock mass collected in each cut is recorded in the second column of Table 5 to a precision of 0.1 g, which is realistic in view of possible material losses.

The third and fifth columns of Table 5 report the total ^{241}Am and ^{241}Pu activities recovered from the injection distribution plates and from each milling cut. Note that 6% to 7% of the injected quantities of both ^{241}Pu and ^{241}Am were deposited on the solution distribution plate. Fortuitously, each of the first few cuts was shallower than the planned 2 mm, as evidenced by the total rock mass collected in each of these cuts.

Table 5. Raw results of destructive analysis of E-Core

Cut Number	Rock Mass (g)	Am (μCi)	Am (%)	Pu (μCi)	Pu (%)
Distribution Plate	0.0	1.8	7.0	0.7	6.2
1	5.53	15.4	60.2	4.5	39.8
2	12.96	0.6	2.5	2.2	19.5
Wall #1	14.92	0.8	2.9	0.7	6.2
3	20.68	0.1	0.4	0.1	0.9
4	14.39	8×10^{-2}	0.3	0.1	0.9
5	14.39	5×10^{-3}	0.0	5×10^{-4}	0.0
6	14.18	3×10^{-3}	0.0	2×10^{-4}	0.0
7	36.98	3×10^{-3}	0.0	6×10^{-4}	0.0
8	40.70	3×10^{-3}	0.0	7×10^{-4}	0.0
Wall #2	28.41	1×10^{-2}	0.0	2×10^{-3}	0.0
Totals	203.14	18.8	73.4	8.3	73.5

Approximately 73% of each of the injected ^{241}Pu and the injected ^{241}Am were recovered from the distribution plate and in the top few millimeters of the core, including the annular cuts. Indeed, only a miniscule quantity of either actinide was recovered in cuts after the fourth vertical cut, even though the majority of the rock was milled in the fifth through eighth cuts.

INTERPRETATION OF ANALYSIS RESULTS

Actinide Concentration Profiles

In order to estimate transport parameters such as retardation factors R and geochemical distribution coefficients K_d as defined, for example, by Fetter (1993), it is necessary to convert the raw data of Table 5 to actinide concentration profiles as functions of depth. As appropriate, these concentration profiles can then be compared with the results of transport calculations using the single-porosity version of COLUMN 1.4. Thus, the conceptual model for these calculations assume single-porosity flow and transport and a linear adsorption isotherm. Although both of the assumed conceptual models are at best approximate for flow and transport of strongly retarded species in Culebra dolomite, they have been used as approximations for analysis of column transport data for conservative and weakly-retarded radionuclides, as was discussed in the INTRODUCTION.

As was stated earlier, the initial milling was done on the floor of the solution-injection well (with diameter $d_w = 6.35$ cm and depth $h_w = 0.43$ cm) at the upstream end of the core. As reported in Table 2, the core dry bulk density was estimated at $\rho_b = 2.38$ g/cm³ by Lucero *et al.* (1998). Given the total rock mass, m , for a given cut and the dry bulk density ρ_b , the milled volume, V , for the cut is

$$V = m / \rho_b. \quad (1)$$

Given well diameter d_w , the approximate depth of cut, z , is

$$z = V / [\pi (d_w / 2)^2]. \quad (2)$$

The total activity A_{An} of each actinide recovered from each cut is reported in Table 5, in μCi (microcuries). Lucero *et al.*, (1998, Appendix A) provide conversion factors from activity to total number of moles for each species. For ²⁴¹Am,

$$M_{Am} \text{ (moles)} = 1.21 \times 10^{-9} A_{Am} \text{ (}\mu\text{Ci)}, \quad (3a)$$

and, for ²⁴¹Pu,

$$M_{Pu} \text{ (moles)} = 4.03 \times 10^{-11} A_{Pu} \text{ (}\mu\text{Ci)}. \quad (3b)$$

The average bulk actinide (A_n) concentration in either activity per unit volume or moles per unit volume in a given depth cut is estimated simply by dividing either A_{An} or M_{An} by the recovered rock volume V . For a series of depth cuts at a given diameter, the cumulative depth for n cuts is calculated simply by adding the individual depths,

$$Z_{tot}(n) = \sum z_i \quad (i = 1, \dots, n). \quad (4)$$

For purposes of plotting data (say activity or moles per unit volume vs. depth), the abscissa may be taken as the average depth in each cut,

$$Z_{av}(n) = [Z_{tot}(n) - Z_{tot}(n-1)] / 2, \quad (5)$$

where $Z_{av}(0) \equiv 0$.

In order to reduce the raw data of Table 5 to tables of actinide activity and/or quantity per unit volume vs. depth, Equations (1) through (5) were programmed as a Microsoft Excel

(v. 7.0a) spreadsheet, and the chart production capability of Excel (v. 7.0a) was used to generate plots of the computational results. Computation was carried out using a Hewlett-Packard Kayak XU PC equipped with an Intel 300-MHz Pentium II processor running the Windows NT 4.0 operating system. The Microsoft Excel data spreadsheet is attached as Appendices B and C. The spreadsheet results of calculation are printed in Appendix B, and the formulae are printed in Appendix C. The data in the cells listed in Appendix B were either manually entered or calculated using formulae in corresponding cells of Appendix C.

As mentioned earlier, later cuts in the destructive analysis extended into the walls of the original solution-injection well, thus increasing the well diameter. Thus, the first wall cut removed 14.92 g of rock in an annulus around the original well. Dividing the mass by the estimated density of 2.38 g/cm³, the volume removed was 6.27 cm³. Using the initial well diameter of 6.35 cm, the initial well depth of 0.43 cm, the cumulative depth of the first two cuts of 0.245 cm (see Table 6), for a new well depth of 0.675 cm, and assuming the well remained circular, the new well diameter can be calculated as 7.22 cm. For calculation of cut depths after the first two, 7.22 cm was used as the well diameter.

Table 6. Approximate actinide activity per unit volume as function of depth

Rock Mass (g)	Rock Volume (cm ³)	Depth of Cut (cm)	Cumulative Depth of Cut (cm)	Plot Depth z (cm) ^a	Total Am (μCi)	Bulk Am Conc. (μCi/cm ³)	Total Pu (μCi)	Bulk Pu Conc. (μCi/cm ³)
5.53	2.32	0.073	0.073	0.037	1.54E+01	6.63E+00	4.52E+00	1.95E+00
12.96	5.45	0.172	0.245	0.159	6.36E-01	1.17E-01	2.18E+00	4.00E-01
20.68	8.69	0.212 ^b	0.458	0.351	1.14E-01	1.31E-02	8.85E-02	1.02E-02
14.39	6.05	0.148 ^b	0.605	0.531	7.86E-02	1.30E-02	1.02E-01	1.69E-02
14.39	6.05	0.148 ^b	0.753	0.679	5.00E-03	8.27E-04	4.70E-04	7.77E-05
14.18	5.96	0.146 ^b	0.898	0.826	3.08E-03	5.17E-04	2.44E-04	4.10E-05
36.98	15.54	0.380 ^b	1.278	1.088	3.47E-03	2.23E-04	6.12E-04	3.94E-05
40.70	17.10	0.418 ^b	1.696	1.487	3.14E-03	1.84E-04	6.60E-04	3.86E-05

Notes: a. For purposes of plotting, plot depth z is taken as the mid-depth of each cut.
b. Calculated at increased well diameter of 7.22 cm.

Table 6 summarizes the results of this analysis, the ²⁴¹Am activity per unit rock volume is plotted in Figure 6a, and the ²⁴¹Pu activity per unit rock volume is plotted in Figure 6b. Clearly, the majority of the recovered ²⁴¹Pu and ²⁴¹Am were captured in the top few millimeters of E-Core.

Potential sources of error in the experimental data are lack of complete recovery of actinide-containing rock flour and possible analysis errors associated with the radio-analytic techniques used. For example, as was discussed earlier, suspended rock powder interfered with the γ-ray spectroscopy normally used for ²⁴¹Am analysis, and LSC (of α-particle emission) had to be used for this analysis. Available weighing accuracy and radio-analytic counting accuracy are far higher than is expected for actual recovery of the rock flour, so it is probably permissible to lump analytical inaccuracies into recovery losses.

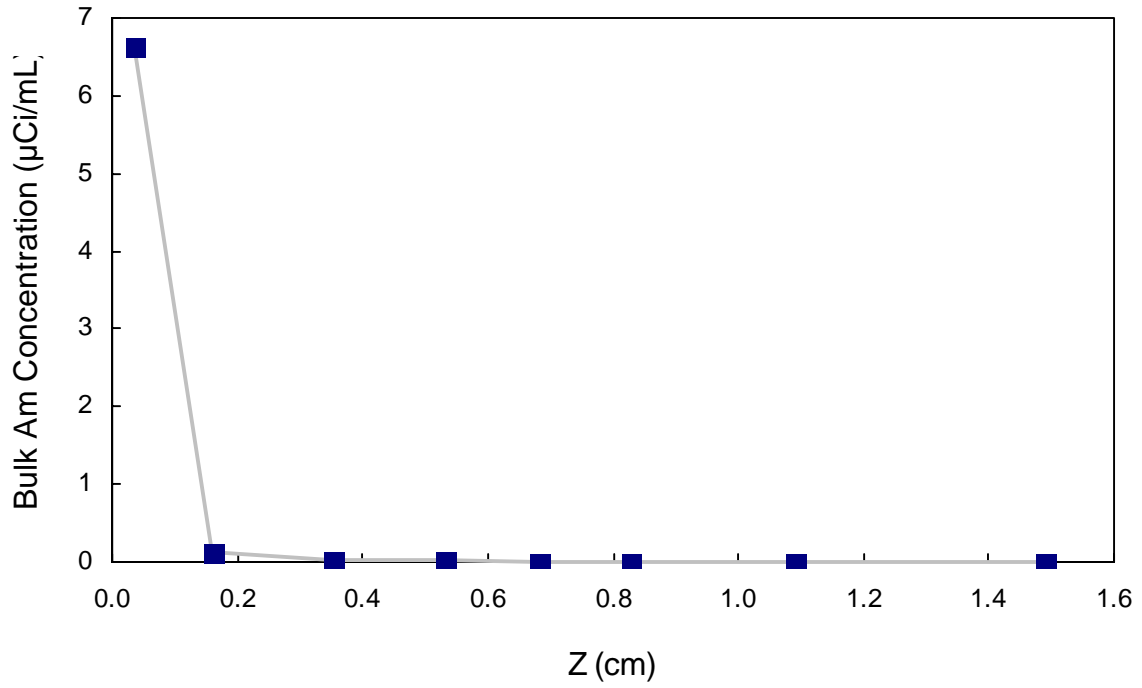


Figure 6a. Measured ^{241}Am activity per unit rock volume as a function of depth.

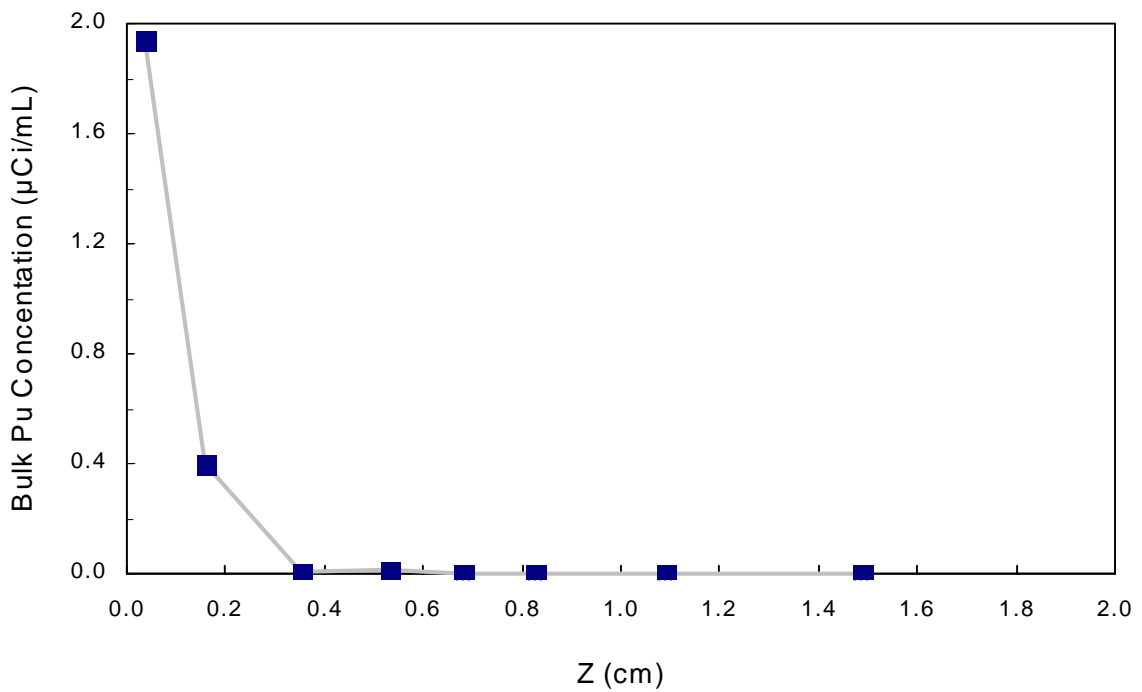


Figure 6b. Measured ^{241}Pu activity per unit rock volume as a function of depth.

Estimation of Retardation Parameters

Attempts to estimate the retardation parameters with the computational tool available (the COLUMN code) are complicated by several factors. First, the brine flow rate was not maintained constant throughout the experiment. As indicated in Table 3, brine flow was begun on December 20, 1995 and maintained at 0.1 mL/min until April 9, 1996, when it was paused until June 4, 1996, on which date flow was started again and maintained at 0.05 mL/min until flow was terminated on July 15, 1996. The initial injection of ^{241}Am and ^{241}Pu was done on January 16, 1996. In addition, a second injection of ^{241}Am (along with live WIPP-relevant microbes) was done on March 22, 1996. Although the COLUMN code has the capability to analyze the effect of multiple input pulses, it does not automatically allow for interruption in brine flow or changes in brine-flow rate.

Because the single-porosity model is linear and also because experimental observations indicate very little migration of either ^{241}Pu or ^{241}Am , it seems reasonable to use eluted brine volume, rather than time, as the independent variable for comparing experimental results to model predictions. Parker and van Genuchten (1984) defined a transformation of variables that permits one to use pore volumes rather than time as the independent variable for the linear equilibrium single-porosity transport equation. Transformation of variables for the E-Core experiments is discussed in Appendix D. Using the transformed variables in COLUMN 1.4 allows one to bridge the inactive period and account for the change in flow rate. The COLUMN 1.4 output provides dissolved actinide concentration as a function of fractional distance through the intact-core column. Calculation of actinide concentration in the rock as a function of depth requires transformations of both the depth and concentration variables. By Equation D-3, the depth variable used for calculation was Z , units of core lengths. Thus, the depth in cm is $z = L Z$, where $L = 10.2$ cm.

For comparison with the analytical results, the calculated dissolved actinide concentration must be transformed to concentration in the rock, C_T . Equation 6, (derived in Appendix E) provides the formula for this transformation.

$$C_T = \theta C_{\text{sol}} R, \quad (6)$$

where θ is the porosity, C_{sol} is the dissolved concentration, and R is the apparent retardation factor.

COLUMN 1.4 uses or creates two input files and generates one or two output files. The first input file is a "*.inp" file that contains two columns. The first column gives z values at which dissolved actinide concentration is to be calculated, and the second column gives a time value for the calculation. Variable z implies fixed time, and variable time requires fixed z . Appendix F contains listings of files "Am_vs_Z_Vol.inp" and "Pu_vs_Z_Vol.inp." The first column of each listing gives depths Z at which dissolved actinide concentration was to be calculated (in units of core length). The second column gives the time at which the calculations were to be performed (in units of pore volume). The data columns in the two files are, of course, identical.

The second COLUMN 1.4 input file is a "*.col" file that contains control information for the calculations to be performed. This information includes a run title, input and output file names, model identification, curve type, parameter values, and information on input

spikes. For this report, two calculations were performed for each actinide, at retardation values of 160,000 and 1,000,000. The four corresponding “*.col” files are listed in Appendix G.

The two COLUMN 1.4 output files are “*.log” and “*.out” files. The “*.log” file contains run identification information from the input “*.col” file as well as computational results. Thus, only the “*.log” files for the four runs are listed in Appendix H.

Finally, Microsoft Excel 97 spreadsheet software was used to transform the COLUMN 1.4 independent variable from dimensionless depth to depth in centimeters. The Excel chart capability was used to co-plot calculational results with experimental measurements of actinide concentration. The Excel 97 spreadsheets and associated graphical charts are listed in Appendix I. For each calculation, Appendix I contains: a spreadsheet with the computational results; an Excel 97 chart that depicts the relation of calculated to observed concentrations; and a spreadsheet that reports formulas used in generating the calculated results. The graphical data are also included as Figures 7, 8, 9, and 10.

As is obvious from Figures 7, 8, 9, and 10, fitting the observed actinide concentration profiles using the single-porosity, linear adsorption-isotherm, one-dimensional code COLUMN 1.4 would be difficult, if not impossible. Several potential reasons exist for this failure to fit, the most obvious of which is that the conceptual models on which this code is based are probably too simple to account for the geochemistry that occurs for very high retardation coefficients. However, it is also clear that effective retardation values greater than 1×10^5 are consistent with the observed experimental data for both ^{241}Am and ^{241}Pu .

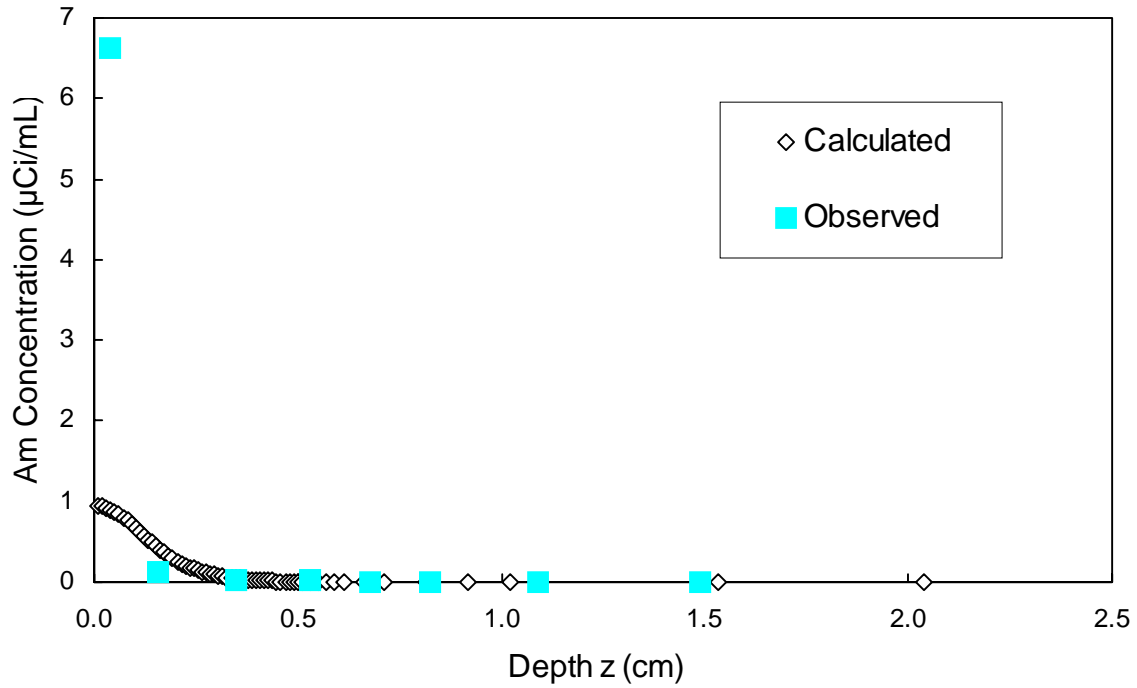


Figure 7. Comparison of measured ^{241}Am activity per unit rock volume to results of calculation for retardation factor $R = 160,000$.

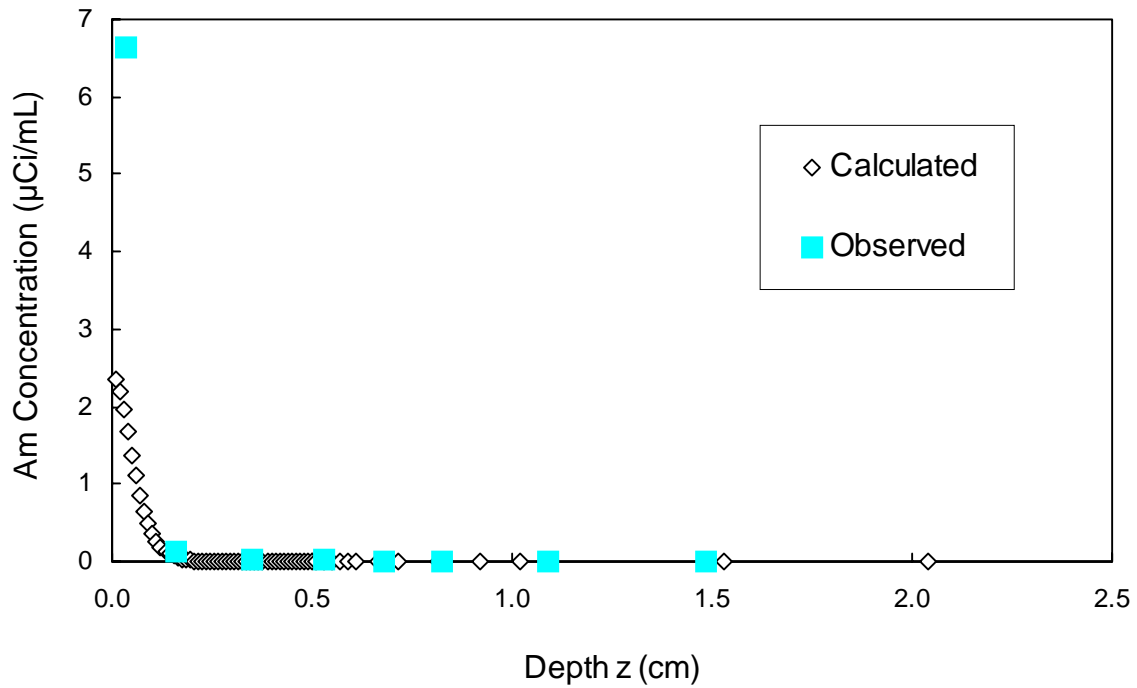


Figure 8. Comparison of measured ^{241}Am activity per unit rock volume to results of calculation for retardation factor $R = 1,000,000$.

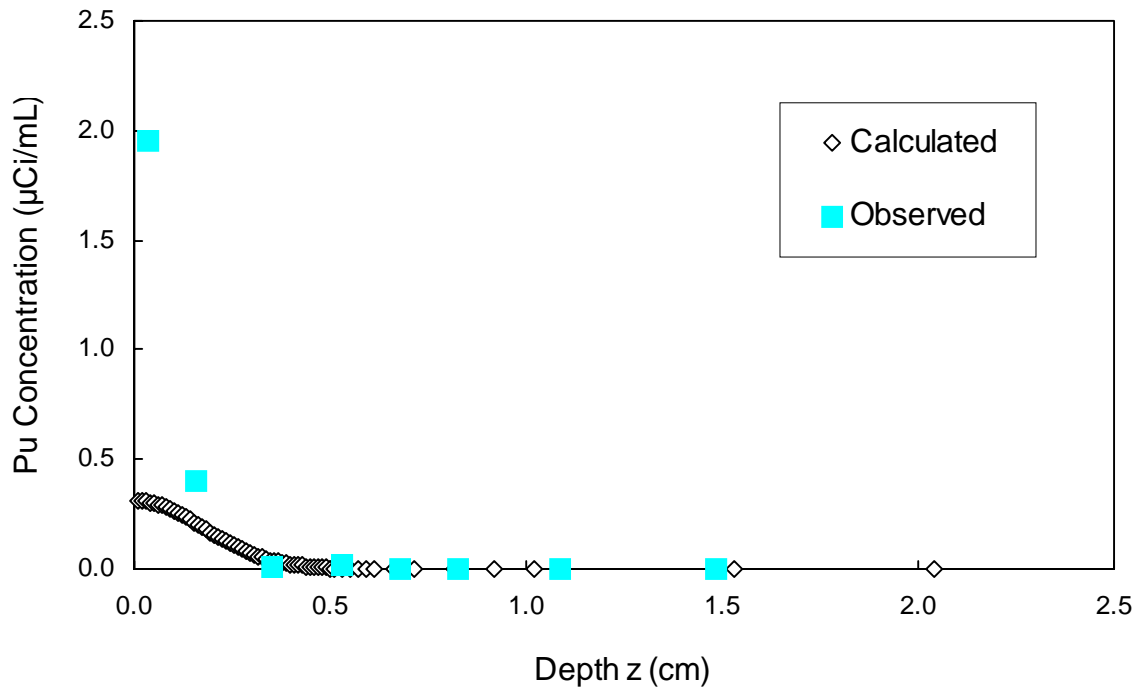


Figure 9. Comparison of measured ^{241}Pu activity per unit rock volume to results of calculation for retardation factor $R = 160,000$.

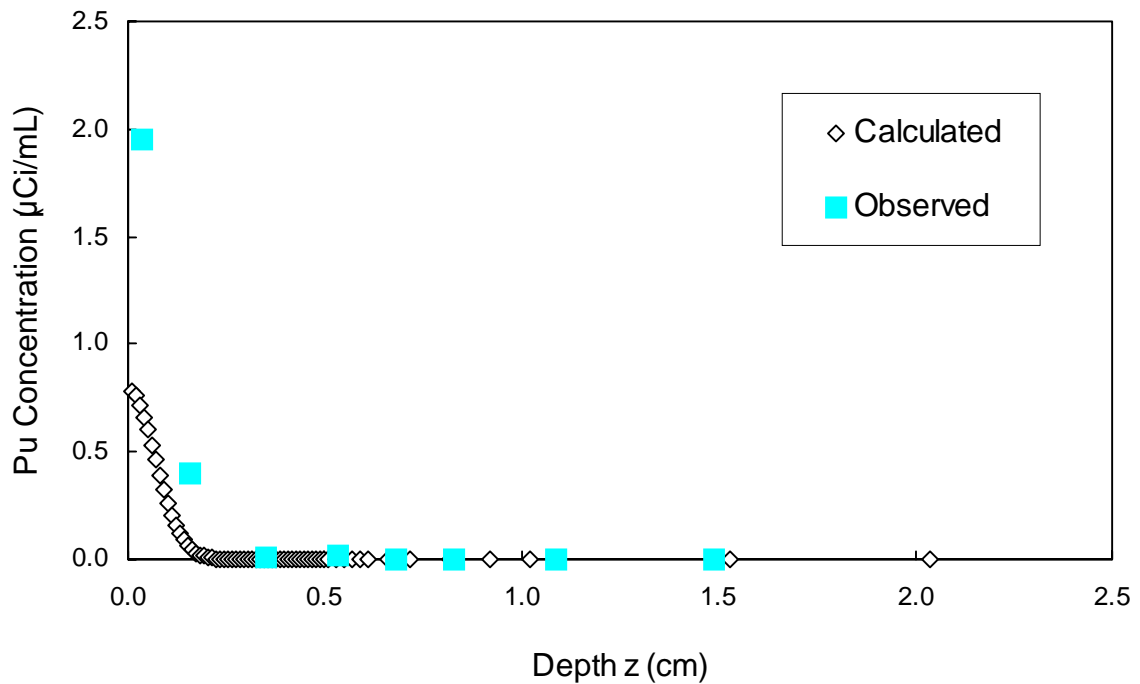


Figure 10. Comparison of measured ^{241}Pu activity per unit rock volume to results of calculation for retardation factor $R = 1,000,000$.

DISCUSSION

We have attempted to use the COLUMN one-dimensional flow and transport code in its single-porosity mode to obtain estimates of retardation and distribution parameters that would be consistent with the curves displayed in Figures 6a and 6b. However, even for the very high retardation constants, the calculated depth of penetration of the actinides exceeds that which is observed.

In the case of ^{241}Am , it is probable that the injected actinide precipitated near the entry surface of the core. At the time of ^{241}Pu and ^{241}Am injection into E-Core (early 1996), solubility models for these species in Culebra brine were still under development. Later, Craft and Siegel (1998) calculated solubility values for Am^{3+} and other actinide species in an air-intake-shaft brine simulant. Calculated solubilities at atmospheric CO_2 pressure were 6.46×10^{-9} M (pmH = 7.73, without dolomite equilibrium) and 9.63×10^{-9} M (pmH = 7.64, with dolomite equilibrium). The input ^{241}Am spike activity for test E-2 was $0.66 \mu\text{Ci/mL}$ (8.0×10^{-7} M), which was thus supersaturated by a factor of at least 83.1 ($8.0 \times 10^{-7}/9.63 \times 10^{-9}$). Similarly, the second ^{241}Am spike activity (for test E-2) was $0.67 \mu\text{Ci/mL}$ (8.1×10^{-7} M), which was thus supersaturated by a factor of at least 84.1 ($8.1 \times 10^{-7}/9.63 \times 10^{-9}$). For both ^{241}Am spikes, the degree of supersaturation was such that it is likely that the majority of the ^{241}Am precipitated at or near the core top surface, consistent with the observed ^{241}Am profile, which is strongly peaked near the injection surface.

Almost certainly, the dissolved ^{241}Am oxidation state was Am^{3+} . The ^{241}Pu oxidation state is not so well-defined. A ^{241}Pu solution in 1 M HCl was submitted to the Los Alamos National Laboratory Chemical Science and Technology Division for oxidation-state determination in December 1994. The response from Los Alamos is included as Appendix J. From the discussion in the Los Alamos report, it could be argued that ^{241}Pu might have been present as either Pu^{4+} or Pu^{5+} or even as a mixture of these oxidation states. One would expect the solubility of Pu^{5+} to be similar to that for Np^{5+} , reported by Craft and Siegel (1998) as 7.84×10^{-6} M (pmH = 7.72, without dolomite equilibrium) and 1.1×10^{-5} M (pmH = 7.64, with dolomite equilibrium). Similarly, one would expect the solubility of Pu^{4+} to be similar to that for Th^{4+} , reported by Craft and Siegel (1998) as 1.9×10^{-7} (pmH = 7.73, without dolomite equilibrium) and 1.57×10^{-7} (pmH = 7.64, with dolomite equilibrium). The input ^{241}Pu spike activity for test E-2 was $0.61 \mu\text{Ci/mL}$ (2.5×10^{-8} M), which appears not to be saturated with respect to either 4+ or 5+ solubility.

Given that the ^{241}Pu should have been soluble under the intact-core column experimental conditions, one would, perhaps, expect better agreement between calculated and observed concentration profiles in Figure 9 or Figure 10. However, even for a dissolved species, it is worth noting that the model assumptions (single-porosity, linear adsorption isotherm, one-dimensional transport) on which COLUMN is based may not be appropriate for very high retardation values.

Potential sources of error in numerical analyses of the data are primarily failure to transfer data correctly, failure properly to encode formulas used into the Excel spreadsheets, and failure to construct appropriate position-time and parameter input files for COLUMN 1.4 calculations. These potential errors have been minimized by including details of the

calculations and results as Appendices B, C, F, G, and I of this report, which have been subjected to technical and QA reviews by qualified reviewers.

As mentioned in the section on interpretation of analysis results, potential sources of error in the experimental data are lack of complete recovery of actinide-containing rock flour and possible analysis errors associated with the radio-analytic techniques used. For example, suspended rock powder interfered with the γ -ray spectroscopy normally used for ^{241}Am analysis, and LSC (of α -particle emission) had to be used for this analysis.

Available weighing accuracy and radio-analytic counting accuracy are far higher than is expected for actual recovery of the rock flour, so it is probably permissible to lump the analytical inaccuracies into recovery losses.

CONCLUSIONS

Using results of single-porosity modeling uncritically, we could argue from the data and computational plots of Figures 7 and 8 that the retardation, $R \approx 1 \times 10^6$, for ^{241}Am . Similarly, we could argue from the plots of Figures 9 and 10 that, for ^{241}Pu ,

$$1.6 \times 10^5 < R < 1 \times 10^6.$$

In view of the probable ^{241}Am precipitation discussed earlier, it is conservative to assert that the destructive analysis results support retardation values,

$$R > 1 \times 10^5,$$

for both species ^{241}Am and ^{241}Pu . For the linear isotherm approximation (Fetter, 1993)

$$R = 1 + (\rho_b K_d / \theta), \quad (7)$$

where ρ_b is the rock bulk density (about 2.4 g/cm^3 for the Culebra dolomite), K_d is the distribution coefficient between dissolved and sorbed actinide (cm^3/g), and θ is the rock porosity (fitted for E-Core at 0.21 – see Appendix D and Lucero *et al.*, 1998). Solving Equation (7) for K_d and inserting the parameter values given here yields

$$K_d = (R - 1) \theta / \rho_b, \quad (8)$$

$$K_d = (10^5 - 1) (0.21) / (2.4) = 8,750.$$

Sensitivity analyses performed for the WIPP (Blaine, 1997) have indicated that, even for worst-case scenarios, K_d values greater than 3 are adequate to prevent violation of the EPA standards for release of radionuclides to the accessible environment. Clearly, then, K_d values on the order of 10^3 or 10^4 are more than adequate to prevent violation of the EPA standards.

REFERENCES

- Behl, Y. K., and D. A. Lucero, 1996. *Test Plan for Laboratory Column Experiments for Radionuclide Adsorption Studies of the Culebra Dolomite Member of the Rustler Formation at the WIPP Site: Test Plan Addendum – Post-Test Core Evaluation*, SNL Test Plan Addendum to TP 95-03, Effective Date 12/10/96, Sandia National Laboratories, Albuquerque, NM.
- Blaine, R. L., 1997. *Expedited CCA Activity – Evaluation of Minimum K_d Parameter Values for Culebra Transport*, WPO #41944, Sandia National Laboratories, Albuquerque, NM, January 24, 1997.
- Brown, G. O., H.-T. Hsieh, and Y.-W. Lin, 1997. *COLUMN: A Computer Program for Fitting Model Parameters to Column Flow Breakthrough Curves, Version 1.4 for Windows 95/NT3.51/NT4.0*, WPO #46281, Sandia National Laboratories, Albuquerque, NM, June 13, 1997.
- Brush, L. H., 1996. “Ranges and Probability Distributions of K_{ds} for Dissolved Pu, Am, U, Th, and Np in the Culebra for the PA Calculations to Support the WIPP CCA,” Memorandum to M. S. Tierney, dated June 10, 1996. Albuquerque, NM: Sandia National Laboratories. (Copy on file in the Sandia WIPP Central Files, Sandia National Laboratories, Albuquerque, NM as WPO#38801).
- Budge, K. G., 1996. *COLUMN: A Computer Program for Fitting Model Parameters to Column Flow Breakthrough Curves, Version 1.3*, WPO #37867, Sandia National Laboratories, Albuquerque, NM.
- Craft, C. C., and M. D. Siegel, 1997. “Additional Calculations of Solubility-Limited Concentrations of Actinides for Injection Spikes used in the WIPP Core Column Experiments at Sandia National Laboratories,” Memorandum to D. Lucero, dated June 9, 1997. Sandia National Laboratories, Albuquerque, NM [Copy on file in the Sandia WIPP Central Files in Lucero, 1995-1997, WPO #40975].
- Fetter, C. W., 1993. *Contaminant Hydrogeology*, pp. 117-119, Upper Saddle River, NJ: Prentice Hall.
- Holt, R. M., 1997. *Conceptual Model for Transport Processes in the Culebra Dolomite Member, Rustler Formation*. SAND97-0194. Albuquerque, NM: Sandia National Laboratories.
- Lucero, D. A., 1995-1997. *WIPP Laboratory Notebooks*, Notebook Number 100396, Entry Dates 10/3/96 through 5/6/97, WPO #40975, Multiple Volumes, WIPP Central Files, Sandia National Laboratories, Albuquerque, NM.
- Lucero, D. A., F. Gelbard, Y. K. Behl, and J. A. Romero, 1995. *Test Plan for Laboratory Column Experiments for Radionuclide Adsorption Studies of the Culebra Dolomite Member of the Rustler Formation at the WIPP Site*, SNL Test Plan TP 95-03, Sandia National Laboratories, Albuquerque, NM.

- Lucero, D. A., G. O. Brown, and C. E. Heath, 1997. *Laboratory Column Experiments for Radionuclide Adsorption Studies of the Culebra Dolomite Member of the Rustler Formation*, SAND97-1763, Sandia National Laboratories, Albuquerque, NM.
- Meigs, L. C., R. L. Beauheim, J. T. McCord, Y. W. Tsang, and R. Haggerty, 1997. "Design, Modeling, and Current Interpretations of the H-19 and H-11 Tracer Tests at the WIPP Site," in *Field Tracer Transport Experiments, Proceedings of the First GEOTRAP Workshop, Cologne, Germany, Aug. 28-30, 1996*.
- Parker, J. C., and M. Th. Van Genuchten, 1984. "Determining Transport Parameters from Laboratory and Field Tracer Experiments," Virginia Agricultural Experimental Station, *Bulletin 84-3*, Virginia Polytechnic Institute and State University, Blacksburg, VA.
- Perkins, W. G., 1998. *Numerical Analysis of Data Obtained from Destructive Analysis of Culebra Intact-Core Columns*, SNL Analysis Plan AP-043, Rev. 00, Sandia National Laboratories, Albuquerque, NM, Effective 3/17/98.
- Public Law 96-164, 1979. *Department of Energy National Security and Military Applications of Nuclear Energy Authorization Act of 1980*. (93 Statute 1259)
- Sandia National Laboratories, 1996, 1997. "Waste Isolation Pilot Plant Quality Assurance Procedure (QAP) 19-1: Computer Software Requirements," effective 9/13/96 and Interim Change Notices 01 (dated 11/14/96), 02 (dated 2/6/97), and 03 (dated 6/19/97).
- U.S. DOE (Department of Energy), 1996. *Waste Isolation Pilot Plant Compliance Certification Application, 40 CFR 191 Subpart B and C*, Carlsbad, NM, October 1996.
- U.S. EPA (Environmental Protection Agency), 1993. "40 CFR Part 191 Environmental Radiation Protection Standards for the Management and Disposal of Spent Nuclear Fuel, High-Level and Transuranic Radioactive Wastes; Final Rule," *Federal Register*. Vol. 58, no. 242, 66,398 – 66,416.

APPENDIX A

**MICROSOFT EXCEL SPREADSHEET OF RAW LIQUID SCINTILLATION
COUNTING DATA**

Count	Mass (gm)	Am241 (uc/gram)	Pu241 (uc/gram)	WALDI (cpm)	Mass (gm)	Am241 (uc/gram)	Pu241 (uc/gram)	WALDI (cpm)	Mass (gm)	Am241 (uc/gram)	Pu241 (uc/gram)	WALDI (cpm)	Mass (gm)	Am241 (uc/gram)	Pu241 (uc/gram)	WALDI (cpm)	Mass (gm)	Am241 (uc/gram)	Pu241 (uc/gram)	WALDI (cpm)	Mass (gm)	Am241 (uc/gram)	Pu241 (uc/gram)	WALDI (cpm)			
1	6.21	2.56E-01	6.89E-02	118	5.44	2.26E-02	4.45E-02	187	5.75	0	0	0	191	6.04	6.02E-03	2.97E-03	208	6.12	3.01E-04	3.14E-05	208	6.12	3.01E-04	3.14E-05			
2	4.86	2.26E-01	3.53E-02	118	5.92	1.30E-02	4.87E-02	188	6.42	3.69E-03	5.31E-04	192	6.04	4.32E-03	6.13E-03	207	4.99	2.92E-04	2.71E-05	208	6.14	3.08E-04	4.35E-05				
3	4.76	2.27E-01	4.17E-02	120	6.22	1.78E-02	1.02E-02	188	6.27	4.90E-03	6.63E-04	193	6.28	6.91E-03	2.74E-03	208	6.14	3.08E-04	4.35E-05	208	6.14	3.08E-04	4.35E-05				
4	4.78	2.34E-01	3.73E-02	121	6.08	2.34E-02	1.18E-02	170	6.1	3.23E-03	5.63E-04	184	4.92	2.99E-03	6.23E-03	208	6.03	2.86E-04	2.71E-05	208	6.03	2.86E-04	2.71E-05				
5	5	2.32E-01	2.67E-02	122	6.53	1.25E-02	3.69E-02	171	4.96	1.46E-02	1.10E-02	185	4.7	2.73E-03	6.32E-03	210	6.28	3.12E-04	2.39E-05	210	6.28	3.12E-04	2.39E-05				
6	4.05	1.79E-01	2.58E-02	123	6.24	1.18E-02	1.87E-02	172	4.84	1.52E-02	1.20E-02	188	5.32	2.99E-03	6.86E-03	211	6.42	2.85E-04	2.19E-05	211	6.42	2.85E-04	2.19E-05				
7	4.86	2.35E-01	4.04E-02	123	6.5	1.90E-02	1.81E-02	173	4.85	1.50E-02	6.89E-03	187	6.25	4.12E-03	3.00E-03	212	6.48	2.71E-04	3.84E-05	212	6.48	2.71E-04	3.84E-05				
8	5.02	2.54E-01	6.83E-02	124	6.01	1.77E-02	3.70E-02	174	4.84	1.31E-02	6.67E-03	188	6.04	3.82E-03	3.70E-03	213	6.01	2.86E-04	2.40E-05	213	6.01	2.86E-04	2.40E-05				
9	5.11	2.39E-01	1.95E-01	125	6.07	1.90E-02	1.69E-02	175	4.89	6.12E-03	2.20E-03	189	6.19	4.29E-03	2.20E-03	214	6.36	2.86E-04	2.40E-05	214	6.36	2.86E-04	2.40E-05				
10	4.92	2.38E-01	6.56E-02	126	6.14	1.67E-02	1.09E-02	176	4.92	1.39E-02	7.50E-03	180	6.34	4.01E-03	1.81E-03	215	4.81	2.51E-04	2.21E-05	215	4.81	2.51E-04	2.21E-05				
11	4.87	2.34E-01	5.34E-02	127	6.49	2.28E-02	1.81E-02	177	6.44	8.82E-03	6.02E-03	181	4.77	2.46E-03	2.65E-03	219	4.78	2.63E-04	1.93E-05	219	4.78	2.63E-04	1.93E-05				
12	4.73	2.32E-01	4.81E-02	128	6.03	1.93E-02	2.42E-02	178	6.08	9.21E-03	2.84E-02	182	6.14	3.80E-03	6.12E-03	217	4.8	2.48E-04	2.34E-05	217	4.8	2.48E-04	2.34E-05				
13	4.68	2.32E-01	4.17E-02	130	6.1	2.00E-02	2.55E-02	178	6.05	8.42E-03	2.68E-02	183	6.05	8.42E-03	2.68E-02	218	4.88	2.48E-04	2.30E-05	218	4.88	2.48E-04	2.30E-05				
14	4.84	2.30E-01	4.01E-02	131	6.29	1.78E-02	1.82E-02	179	6.05	8.42E-03	2.68E-02	183	4.87	4.31E-03	2.62E-03	219	4.88	2.48E-04	2.30E-05	219	4.88	2.48E-04	2.30E-05				
15	4.94	2.49E-01	4.85E-02	132	4.99	1.88E-02	1.87E-02	180	16.48	0.00E+00	0.00E+00	184	6.06	4.66E-03	7.38E-03	219	4.88	2.48E-04	2.30E-05	219	4.88	2.48E-04	2.30E-05				
16	4.89	2.53E-01	4.11E-02	132	6.02	1.76E-02	2.28E-02	185	6.11	4.34E-03	6.60E-03	220	6.23	2.78E-04	2.78E-04	240E-05	240E-05	240E-05	240E-05	240E-05	240E-05	240E-05	240E-05	240E-05	240E-05		
17	4.88	2.37E-01	1.05E-01	134	6.3	1.63E-02	1.61E-02	186	6.06	4.83E-03	6.74E-03	221	6.19	2.30E-04	1.09E-04	240E-05	240E-05	240E-05	240E-05	240E-05	240E-05	240E-05	240E-05	240E-05	240E-05		
18	4.89	2.38E-01	6.85E-02	134	6.18	1.98E-02	2.71E-02	187	6.18	2.21E-03	1.03E-02	222	6.18	2.21E-03	1.03E-02	240E-05	240E-05	240E-05	240E-05	240E-05	240E-05	240E-05	240E-05	240E-05	240E-05		
19	5.15	2.49E-01	6.47E-02	135	6.08	1.68E-02	2.97E-02	188	6.08	2.92E-03	1.36E-02	222	6.14	2.81E-03	6.10E-03	223	6.55	2.58E-04	2.39E-05	223	6.55	2.58E-04	2.39E-05	223	6.55	2.58E-04	2.39E-05
20	4.94	2.34E-01	5.75E-02	137	5.4	1.62E-02	1.48E-02	188	6.04	1.44E-03	6.48E-03	224	6.04	1.44E-03	6.48E-03	224	5.11	1.54E-04	1.71E-05	224	5.11	1.54E-04	1.71E-05	224	5.11	1.54E-04	1.71E-05
21	4.99	2.31E-01	4.98E-02	138	6.41	1.85E-02	1.48E-02	188	6.41	1.85E-02	1.48E-02																
22	5.13	2.46E-01	4.83E-02	138	6.23	1.85E-02	1.44E-02	188	6.23	1.85E-02	1.44E-02																
23	4.72	2.17E-01	4.20E-02	140	6.2	1.71E-02	7.84E-03	188	6.2	1.71E-02	7.84E-03																
24	4.8	2.24E-01	5.84E-02	141	6.29	1.85E-02	1.00E-02	188	6.29	1.85E-02	1.00E-02																
25	4.77	2.24E-01	5.84E-02	142	6.03	2.16E-02	6.82E-02	188	6.03	2.16E-02	6.82E-02																
26	5.06	2.38E-01	5.52E-02	143	5.13	1.62E-02	1.36E-02	188	5.13	1.62E-02	1.36E-02																
27	4.81	2.21E-01	4.85E-02	144	6.19	1.24E-02	6.60E-03	188	6.19	1.24E-02	6.60E-03																
28	4.99	2.32E-01	4.83E-02	145	6.35	1.66E-02	4.16E-02	145	6.35	1.66E-02	4.16E-02																
29	4.88	2.05E-01	3.70E-02	145	5.49	1.59E-02	1.20E-02	148	5.49	1.59E-02	1.20E-02																
30	4.88	3.31E-01	3.00E-01	147	6.31	1.75E-02	2.01E-02	147	6.31	1.75E-02	2.01E-02																
31	4.89	1.80E-01	4.00E-02	148	6.31	2.08E-02	1.87E-02	148	6.31	2.08E-02	1.87E-02																
32	5.09	1.64E-01	4.91E-02	149	5.28	1.42E-02	6.05E-03	149	5.28	1.42E-02	6.05E-03																
33	4.97	1.44E-01	3.86E-02	150	6.48	7.98E-03	4.23E-02	150	6.48	7.98E-03	4.23E-02																
34	5	1.49E-01	4.24E-02	151	6.62	1.54E-02	1.40E-02	151	6.62	1.54E-02	1.40E-02																
35	5.04	1.59E-01	4.28E-02	152	6.45	1.45E-02	1.22E-02	152	6.45	1.45E-02	1.22E-02																
36	4.81	1.31E-01	3.00E-02	153	5.2	1.82E-02	9.70E-03	153	5.2	1.82E-02	9.70E-03																
37	4.98	3.24E-01	2.22E-01	154	6.26	1.65E-02	9.68E-03	154	6.26	1.65E-02	9.68E-03																
38	5.21	2.35E-01	1.18E-01	155	6.08	6.02E-03	3.38E-02	155	6.21	1.63E-02	1.16E-02	155	6.21	1.63E-02	1.16E-02												
39	4.97	2.10E-01	1.46E-01	156	6.33	5.76E-03	2.47E-02	156	6.33	5.76E-03	2.47E-02																
40	4.78	2.96E-01	2.87E-01	157	6.34	1.18E-02	9.82E-03	157	6.34	1.18E-02	9.82E-03																
41	5.18	8.95E-01	1.22E-01	158	5.48	1.19E-02	1.28E-02	158	5.48	1.19E-02	1.28E-02																
42	4.99	9.26E-01	1.93E-01	159	6.61	3.32E-02	2.08E-02	159	6.61	3.32E-02	2.08E-02	159	6.61	3.32E-02	2.08E-02	159	6.61	3.32E									

APPENDIX B

**MICROSOFT EXCEL SPREADSHEET USED TO CALCULATE ACTINIDE
CONCENTRATION VS. DEPTH RESULTS OF CALCULATION**

	A	B	C	D	E	F	G	H	I	J	K	L	M
34	Calculation of well diameter after first wall cut:												
35	Assumes rock density: 2.38 g/cm ³ , initial well diameter (d0) 6.35 cm, initial well depth 0.43 cm,												
36	Wall mass (14.92 g) removed after cumulative depth of 0.245 cm beyond initial well bottom.												
37													
38		Mass	14.92										
39		V(tot)	6.27										
40		h	0.68										
41		r(0)	3.18										
42		d(0)	6.35										
43		r(1)	3.61										
44		d(1)	7.22										
45													
46	Calculation of annulus depth after second wall cut:												
47	Assumes rock density: 2.38 g/cm ³ , second well diameter (d1) 7.22 cm, well radius increased by												
48	0.8 cm. Wall mass of 28.41γ removed in annulus at top surface to a depth to be determined.												
49													
50		Mass	28.41										
51		V(tot)	11.94										
52		r(1)	3.61										
53		d(1)	7.22										
54		r(2)	4.41										
55		d(2)	8.82										
56		h(ann)	0.59										

APPENDIX C

**MICROSOFT EXCEL SPREADSHEET USED TO CALCULATE ACTINIDE
CONCENTRATION VS. DEPTH FORMULAS**

	I	J	K	L	M
1					
2					
3					
4	Total	Bulk Am		Bulk Pu	Bulk Pu
5	Am	Conc		Conc	Conc
6	(mol)	(mol/mL)		(mCi/mL)	(mol/mL)
7	=G7*0.00000000121	=H7*0.00000000121		=G22/C22	=H22*0.000000000403
8	=G8*0.00000000121	=H8*0.00000000121		=G23/C23	=H23*0.000000000403
9	=G9*0.00000000121	=H9*0.00000000121		=G24/C24	=H24*0.000000000403
10	=G10*0.00000000121	=H10*0.00000000121		=G25/C25	=H25*0.000000000403
11	=G11*0.00000000121	=H11*0.00000000121		=G26/C26	=H26*0.000000000403
12	=G12*0.00000000121	=H12*0.00000000121		=G27/C27	=H27*0.000000000403
13	=G13*0.00000000121	=H13*0.00000000121		=G28/C28	=H28*0.000000000403
14	=G14*0.00000000121	=H14*0.00000000121		=G29/C29	=H29*0.000000000403
15	=G15*0.00000000121	=H15*0.00000000121		=G30/C30	=H30*0.000000000403
16	=G16*0.00000000121	=H16*0.00000000121		=G31/C31	=H31*0.000000000403
17	=G17*0.00000000121				
18					
19	Total	Bulk Pu			
20	Pu	Conc			
21	(mol)	(mol/mL)			
22	=G22*0.000000000403	=H22*0.000000000403			
23	=G23*0.000000000403	=H23*0.000000000403			
24	=G24*0.000000000403	=H24*0.000000000403			
25	=G25*0.000000000403	=H25*0.000000000403			
26	=G26*0.000000000403	=H26*0.000000000403			
27	=G27*0.000000000403	=H27*0.000000000403			
28	=G28*0.000000000403	=H28*0.000000000403			
29	=G29*0.000000000403	=H29*0.000000000403			
30	=G30*0.000000000403	=H30*0.000000000403			
31	=G31*0.000000000403	=H31*0.000000000403			
32	=G32*0.000000000403				
33					

	A	B	C	D	E	F	G	H
34								
35								
36								
37								
38		Mass	14.92					
39		V(tot)	=C38/2.38					
40		h	=0.43 + 0.245					
41		r(0)	=6.35/2					
42		d(0)	6.35					
43		r(1)	=SQRT(C39/(C40*PI()) + C41^2)					
44		d(1)	=2*C43					
45								
46								
47								
48								
49								
50		Mass	28.41					
51		V(tot)	=C50/2.38					
52		r(1)	=C43					
53		d(1)	=C44					
54		r(2)	=C52+0.8					
55		d(2)	=2*C54					
56		h(ann)	=C51/(PI()*(C54^2 - C52^2))					

APPENDIX D

DIMENSIONLESS FORM OF LINEAR-EQUILIBRIUM TRANSPORT EQUATION FOR E-CORE EXPERIMENTS

Development of Dimensionless Equations

The basic linear-equilibrium transport equation is

$$R \frac{\partial C}{\partial t} = D \frac{\partial^2 C}{\partial z^2} - v \frac{\partial C}{\partial z}, \quad (\text{D-1})$$

where C is the concentration of solute in brine solution, R is the solute retardation coefficient as defined, for example, by Fetter (1993), D is the dispersion coefficient for transport in the medium, t is time, z is distance, $v = q/\theta$ is the average pore water velocity, q is the specific discharge (volumetric flow rate divided by cross-sectional area), and θ is the porosity. For the experiments described here, the initial condition is $C(z,0) = 0$, the boundary condition for $t = 0$, $z = 0$ is a spike of concentration C_0 for duration t_0 , and brine flow is maintained for a time t_{end} . For a column of length L , following Parker and van Genuchten (1984), we define dimensionless variables

$$T = v t/L \text{ (units of pore volumes)} \quad (\text{D-2})$$

$$Z = z/L \text{ (units of core lengths)}. \quad (\text{D-3})$$

Now,

$$\frac{\partial C}{\partial t} = (\partial T/\partial t) (\partial C/\partial T) = (v/L) (\partial C/\partial T),$$

$$\frac{\partial C}{\partial z} = (1/L) (\partial C/\partial Z),$$

and

$$\frac{\partial^2 C}{\partial z^2} = (1/L^2) (\partial^2 C/\partial Z^2).$$

Thus, the transport equation (D-1) becomes

$$R (v/L) (\partial C/\partial T) = (D/L^2) (\partial^2 C/\partial Z^2) - (v/L) (\partial C/\partial Z), \quad (\text{D-4})$$

or

$$R (\partial C/\partial T) = (1/L) (D/v) (\partial^2 C/\partial Z^2) - (\partial C/\partial Z), \quad (\text{D-5})$$

which is in the same form as Eq. (D-1) if the initial parameters are replaced as follows.

$$R^* = R \quad (\text{D-6})$$

$$D^* = (1/L) (D/v) = (1/L) (D\theta/q) \quad (\text{D-7})$$

$$v^* = 1 \quad (\text{D-8})$$

$$q^* = \theta^* \quad (\text{D-9})$$

$$\theta^* = \theta \quad (\text{D-10})$$

$$C_0^* = C_0 \quad (\text{D-11})$$

$$T_0 = (q/\theta L) t_0 \quad (\text{D-12})$$

$$T_{\text{end}} = (q/\theta L) t_{\text{end}} \quad (\text{D-13})$$

Dimensionless Parameter Values

For E-Core (see Table 3), ^{241}Am and ^{241}Pu were first introduced in an 18.5 mL spike at 0.1 mL/min flow rate. The second spike of ^{241}Am was 20 mL at the 0.1 mL/min flow rate. The measured and fitted core parameters reported by Lucero *et al.*, (1998) were:

$$\begin{aligned}
 R &= \text{retardation coefficient (parameter to be fitted)} \\
 q &= 1.009 \times 10^{-5} \text{ cm/s (0.1 mL/min flow rate divided by cross-sectional area)} \\
 L &= 10.2 \text{ cm} \\
 D &= 0.00026 \text{ cm}^2/\text{s (average of fitting parameters for two experiments with } ^{22}\text{Na)} \\
 \theta &= 0.21 \text{ (average of fitting parameters for two experiments with } ^{22}\text{Na)} \\
 t_{01} &= 11,100 \text{ s (for first } ^{241}\text{Pu and } ^{241}\text{Am spike – volume: 18.5 mL)} \\
 C_{01} &= 0.66 \text{ }\mu\text{Ci/mL for first } ^{241}\text{Am spike} \\
 &= 0.61 \text{ }\mu\text{Ci/mL for first } ^{241}\text{Pu spike} \\
 t_{02} &= 12,000 \text{ s (for second } ^{241}\text{Am spike – volume: 20 mL)} \\
 C_{02} &= 0.67 \text{ }\mu\text{Ci/mL (for second } ^{241}\text{Am spike)}.
 \end{aligned}$$

The parameter t_{end} is estimated based on the flow history of the core. The time from first injection of ^{241}Pu and ^{241}Am to the second injection of ^{241}Am was 65 days, and the time from second injection of ^{241}Am to the pause in flow was 18 days. Finally, the time from restart (at half the original flow rate) to end of flow was 41 days (see Lucero *et al.*, 1998). For conversion to pore volumes as the independent variable, the total flow time is taken as:

$$t_{\text{end}} = [(65 + 18 + 41/2) \text{ day}] [86,400 \text{ s/day}] = 8.94 \times 10^6 \text{ s.}$$

This set of parameters transforms to

$$\begin{aligned}
 R^* &= R \\
 D^* &= [(0.00026) (0.21)] / [(1.009 \times 10^{-5}) (10.2)] = 0.53 \\
 \theta^* &= \theta = 0.21 \\
 q^* &= \theta = 0.21 \\
 L^* &= 10.2/10.2 = 1.0 \\
 T_{0n} &= \{(1.009 \times 10^{-5}) / [(0.21) (10.2)]\} t_{0n} = 4.71 \times 10^{-6} t_{0n} \\
 T_{01} &= 0.052 \text{ and } T_{02} = 0.056 \\
 T_{\text{end}} &= 4.71 \times 10^{-6} t_{\text{end}} = 42.1 \text{ (pore volumes)}.
 \end{aligned}$$

Conversion from pore volumes to total volume requires multiplication by core volume and porosity to yield

$$V_{\text{tot}} = \pi (7.25)^2 (10.2) (0.21) T_{\text{end}} = 14.9 \text{ L,}$$

in good agreement with the total volume computed from flow rate and elapsed flow time.

APPENDIX E
DERIVATION OF RELATION BETWEEN
DISSOLVED ACTINIDE CONCENTRATION AND
TOTAL ACTINIDE CONCENTRATION IN THE ROCK

As was stated in the main text, COLUMN 1.4 calculates actinide concentrations in solution, not on the solid. However, for comparison of calculation with the results of destructive analysis, it is necessary to calculate the total concentration of actinide both in solution and sorbed on the rock surfaces. For the approximations is used in this report (i.e., single-porosity and linear sorption isotherm), the sorbed concentration (per unit rock mass) is related to dissolved concentration by the equation

$$S = K_d C_{\text{sol}}, \quad (\text{E-1})$$

where K_d is given in mL/g, and C_{sol} is the dissolved concentration (e.g., $\mu\text{Ci/mL}$). The total volume concentration of actinide (per unit volume of rock) is then

$$C_T = \rho_b S + \theta C_{\text{sol}}, \quad (\text{E-2})$$

where θ is the porosity. Inserting Equation (E-1) into Equation E-2 yields

$$C_T = \rho_b K_d C_{\text{sol}} + \theta C_{\text{sol}} = \theta C_{\text{sol}} [1 + (\rho_b K_d/\theta)]. \quad (\text{E-3})$$

Note that the factor $[1 + (\rho_b K_d/\theta)]$ is just the definition of the retardation factor R . Thus,

$$C_T = \theta C_{\text{sol}} R, \quad (\text{E-4})$$

which, given θ and R , provides a straightforward conversion from dissolved concentration to total concentration in the solid.

APPENDIX F

**LISTINGS OF POSITION-TIME INPUT FILES (*.INP) FOR
COLUMN 1.4 CALCULATIONS**

Am_vs_Z_Vol.inp

0.001 42.1
0.002 42.1
0.003 42.1
0.004 42.1
0.005 42.1
0.006 42.1
0.007 42.1
0.008 42.1
0.009 42.1
0.010 42.1
0.011 42.1
0.012 42.1
0.013 42.1
0.014 42.1
0.015 42.1
0.016 42.1
0.017 42.1
0.018 42.1
0.019 42.1
0.020 42.1
0.021 42.1
0.022 42.1
0.023 42.1
0.024 42.1
0.025 42.1
0.026 42.1
0.027 42.1
0.028 42.1
0.029 42.1
0.030 42.1
0.031 42.1
0.032 42.1
0.033 42.1
0.034 42.1
0.035 42.1
0.036 42.1
0.037 42.1
0.038 42.1
0.039 42.1
0.040 42.1
0.041 42.1
0.042 42.1
0.043 42.1
0.044 42.1
0.045 42.1
0.046 42.1
0.047 42.1
0.048 42.1
0.049 42.1
0.050 42.1
0.052 42.1
0.054 42.1
0.056 42.1

Am_vs_Z_Vol.inp

0.058 42.1
0.060 42.1
0.065 42.1
0.070 42.1
0.080 42.1
0.090 42.1
0.100 42.1
0.150 42.1
0.200 42.1

Pu_vs_Z_Vol.inp

0.001 42.1
0.002 42.1
0.003 42.1
0.004 42.1
0.005 42.1
0.006 42.1
0.007 42.1
0.008 42.1
0.009 42.1
0.010 42.1
0.011 42.1
0.012 42.1
0.013 42.1
0.014 42.1
0.015 42.1
0.016 42.1
0.017 42.1
0.018 42.1
0.019 42.1
0.020 42.1
0.021 42.1
0.022 42.1
0.023 42.1
0.024 42.1
0.025 42.1
0.026 42.1
0.027 42.1
0.028 42.1
0.029 42.1
0.030 42.1
0.031 42.1
0.032 42.1
0.033 42.1
0.034 42.1
0.035 42.1
0.036 42.1
0.037 42.1
0.038 42.1
0.039 42.1
0.040 42.1
0.041 42.1
0.042 42.1
0.043 42.1
0.044 42.1
0.045 42.1
0.046 42.1
0.047 42.1
0.048 42.1
0.049 42.1
0.050 42.1
0.052 42.1
0.054 42.1

Pu_vs_Z_Vol.inp

0.056 42.1
0.058 42.1
0.060 42.1
0.065 42.1
0.070 42.1
0.080 42.1
0.090 42.1
0.100 42.1
0.150 42.1
0.200 42.1

APPENDIX G

LISTINGS OF PARAMETER INPUT FILES (*.COL) FOR COLUMN 1.4 CALCULATIONS

Am160000_vs_Z-Vol.col

[Wcolumn]

Date=4/6/98 3:51:27 PM
Title=Am vs. Depth at R=160,000, two spike input
LogFile=Am160000_vs_Z_Vol.log
OutputFile=Am160000_vs_Z_Vol.out
Model=Linear equilibrium
TracerSpikeType=Multiple
CurveType=Theoretical Curve
Normalization=RESIDENT
Bootstrap=

[DistanceAndTimeSpec.]

Set=File
FileName=Am_vs_Z_Vol.inp

[ParameterValues]

R=160000
theta=0.21
D=0.53
mu=0
gamma=0
q=0.21

[TracerInjections]

NumberOfSpikes= 2
StartTime_1=0
EndTime_1=0.052
Concentration_1=0.66
Adjustable_1=No
StartTime_2=26.451
EndTime_2=26.507
Concentration_2=0.67
Adjustable_2=No

Am1000000_vs_Z-Vol.col

[Wcolumn]

Date=4/6/98 3:51:27 PM
Title=Am vs. Depth at R=1,000,000, two spike input
LogFile=Am1000000_vs_Z_Vol.log
OutputFile=Am1000000_vs_Z_Vol.out
Model=Linear equilibrium
TracerSpikeType=Multiple
CurveType=Theoretical Curve
Normalization=RESIDENT
Bootstrap=

[DistanceAndTimeSpec.]

Set=File
FileName=Am_vs_Z_Vol.inp

[ParameterValues]

R=1000000
theta=0.21
D=0.53
mu=0
gamma=0
q=0.21

[TracerInjections]

NumberOfSpikes= 2
StartTime_1=0
EndTime_1=0.052
Concentration_1=0.66
Adjustable_1=No
StartTime_2=26.451
EndTime_2=26.507
Concentration_2=0.67
Adjustable_2=No

Pu160000_vs_Z-Vol.col

[Wcolumn]

Date=4/6/98 3:52:01 PM

Title=Pu vs. Depth at R=160,000

LogFile=Pu160000_vs_Z_Vol.log

OutputFile=Pu160000_vs_Z_Vol.out

Model=Linear equilibrium

TracerSpikeType=Single

CurveType=Theoretical Curve

Normalization=RESIDENT

Bootstrap=

[DistanceAndTimeSpec.]

Set=File

FileName=Pu_vs_Z_Vol.inp

[ParameterValues]

R=160000

theta=0.21

D=0.53

mu=0

gamma=0

q=0.21

t0=0.052

c0=0.61

Pu100000_vs_Z-Vol.col

[Wcolumn]

Date=4/6/98 3:51:42 PM

Title=Pu vs. Depth at R=1,000,000

LogFile=Pu1000000_vs_Z_Vol.log

OutputFile=Pu1000000_vs_Z_Vol.out

Model=Linear equilibrium

TracerSpikeType=Single

CurveType=Theoretical Curve

Normalization=RESIDENT

Bootstrap=

[DistanceAndTimeSpec.]

Set=File

FileName=Pu_vs_Z_Vol.inp

[ParameterValues]

R=1000000

theta=0.21

D=0.53

mu=0

gamma=0

q=0.21

t0=0.052

c0=0.61

APPENDIX H
LISTINGS OF OUTPUT FILES (*.LOG) FOR
COLUMN 1.4 CALCULATIONS

Am160000_vs_Z_Vol.log

```
*****
*
*   Deterministic linear equilibrium absorption for pulse injection with   *
*   first-order decay                                                    *
*
*   Am vs. Depth at R=160,000, two spike input                          *
*
*****
```

Model Name = Linear equilibrium
Calculation began 4/6/98 3:51:28 PM

Tracer spikes:

Start time	End time	Concentration
0.000000E+00	5.200000E-02	6.600000E-01
2.645100E+01	2.650700E+01	6.700000E-01

Model parameters:

- R = 160000
- theta = 0.21
- D = 0.53
- mu = 0
- gamma = 0
- q = 0.21
- t0 = 0.66
- c0 = 0.67

No fit performed; model calculation only.

Calculated model curves:

Distances	Time	Model
1.000000E-03	4.210000E+01	2.816805E-05
2.000000E-03	4.210000E+01	2.790231E-05
3.000000E-03	4.210000E+01	2.743187E-05
4.000000E-03	4.210000E+01	2.676909E-05
5.000000E-03	4.210000E+01	2.593103E-05
6.000000E-03	4.210000E+01	2.493851E-05
7.000000E-03	4.210000E+01	2.381512E-05
8.000000E-03	4.210000E+01	2.258624E-05
9.000000E-03	4.210000E+01	2.127811E-05
1.000000E-02	4.210000E+01	1.991689E-05
1.100000E-02	4.210000E+01	1.852784E-05
1.200000E-02	4.210000E+01	1.713450E-05
1.300000E-02	4.210000E+01	1.575811E-05
1.400000E-02	4.210000E+01	1.441707E-05
1.500000E-02	4.210000E+01	1.312671E-05
1.600000E-02	4.210000E+01	1.189914E-05
1.700000E-02	4.210000E+01	1.074328E-05
1.800000E-02	4.210000E+01	9.665050E-06
1.900000E-02	4.210000E+01	8.667623E-06
2.000000E-02	4.210000E+01	7.751812E-06
2.100000E-02	4.210000E+01	6.916449E-06
2.200000E-02	4.210000E+01	6.158793E-06
2.300000E-02	4.210000E+01	5.474934E-06
2.400000E-02	4.210000E+01	4.860155E-06
2.500000E-02	4.210000E+01	4.309257E-06
2.600000E-02	4.210000E+01	3.816832E-06
2.700000E-02	4.210000E+01	3.377484E-06
2.800000E-02	4.210000E+01	2.985988E-06
2.900000E-02	4.210000E+01	2.637413E-06
3.000000E-02	4.210000E+01	2.327195E-06
3.100000E-02	4.210000E+01	2.051175E-06
3.200000E-02	4.210000E+01	1.805610E-06
3.300000E-02	4.210000E+01	1.587163E-06

Am160000_vs_Z_Vol.log

3.400000E-02	4.210000E+01	1.392881E-06
3.500000E-02	4.210000E+01	1.220158E-06
3.600000E-02	4.210000E+01	1.066698E-06
3.700000E-02	4.210000E+01	9.304788E-07
3.800000E-02	4.210000E+01	8.097132E-07
3.900000E-02	4.210000E+01	7.028150E-07
4.000000E-02	4.210000E+01	6.083696E-07
4.100000E-02	4.210000E+01	5.251083E-07
4.200000E-02	4.210000E+01	4.518874E-07
4.300000E-02	4.210000E+01	3.876709E-07
4.400000E-02	4.210000E+01	3.316303E-07
4.500000E-02	4.210000E+01	2.826542E-07
4.600000E-02	4.210000E+01	2.401038E-07
4.700000E-02	4.210000E+01	2.032634E-07
4.800000E-02	4.210000E+01	1.714801E-07
4.900000E-02	4.210000E+01	1.441597E-07
5.000000E-02	4.210000E+01	1.207629E-07
5.200000E-02	4.210000E+01	8.383760E-08
5.400000E-02	4.210000E+01	5.736411E-08
5.600000E-02	4.210000E+01	3.867829E-08
5.800000E-02	4.210000E+01	2.569570E-08
6.000000E-02	4.210000E+01	1.681766E-08
6.500000E-02	4.210000E+01	5.455047E-09
7.000000E-02	4.210000E+01	1.607306E-09
8.000000E-02	4.210000E+01	1.139548E-10
9.000000E-02	4.210000E+01	5.449997E-12
1.000000E-01	4.210000E+01	1.821197E-13
1.500000E-01	4.210000E+01	3.493562E-23
2.000000E-01	4.210000E+01	8.530961E-37

Am100000_vs_Z_Vol.log

```
*****
*
*   Deterministic linear equilibrium absorption for pulse injection with   *
*   first-order decay                                                    *
*
*   Am vs. Depth at R=1,000,000, two spike input                        *
*
*****
```

Model Name = Linear equilibrium
Calculation began 4/6/98 5:04:05 PM

Tracer spikes:

Start time	End time	Concentration
0.000000E+00	5.200000E-02	6.600000E-01
2.645100E+01	2.650700E+01	6.700000E-01

Model parameters:

- R = 1000000
- theta = 0.21
- D = 0.53
- mu = 0
- gamma = 0
- q = 0.21
- t0 = 0.66
- c0 = 0.67

No fit performed; model calculation only.

Calculated model curves:

Distances	Time	Model
1.000000E-03	4.210000E+01	1.114651E-05
2.000000E-03	4.210000E+01	1.041313E-05
3.000000E-03	4.210000E+01	9.301828E-06
4.000000E-03	4.210000E+01	7.966166E-06
5.000000E-03	4.210000E+01	6.564837E-06
6.000000E-03	4.210000E+01	5.231721E-06
7.000000E-03	4.210000E+01	4.056345E-06
8.000000E-03	4.210000E+01	3.079880E-06
9.000000E-03	4.210000E+01	2.304260E-06
1.000000E-02	4.210000E+01	1.707177E-06
1.100000E-02	4.210000E+01	1.256265E-06
1.200000E-02	4.210000E+01	9.189481E-07
1.300000E-02	4.210000E+01	6.674512E-07
1.400000E-02	4.210000E+01	4.801959E-07
1.500000E-02	4.210000E+01	3.411962E-07
1.600000E-02	4.210000E+01	2.387381E-07
1.700000E-02	4.210000E+01	1.640962E-07
1.800000E-02	4.210000E+01	1.106656E-07
1.900000E-02	4.210000E+01	7.300206E-08
2.000000E-02	4.210000E+01	4.710155E-08
2.100000E-02	4.210000E+01	2.970249E-08
2.200000E-02	4.210000E+01	1.829581E-08
2.300000E-02	4.210000E+01	1.100234E-08
2.400000E-02	4.210000E+01	6.456136E-09
2.500000E-02	4.210000E+01	3.694751E-09
2.600000E-02	4.210000E+01	2.060980E-09
2.700000E-02	4.210000E+01	1.119851E-09
2.800000E-02	4.210000E+01	5.922775E-10
2.900000E-02	4.210000E+01	3.397494E-10
3.000000E-02	4.210000E+01	1.753675E-10
3.100000E-02	4.210000E+01	8.852817E-11
3.200000E-02	4.210000E+01	4.370556E-11

Am100000_vs_Z_Vol.log

3.300000E-02	4.210000E+01	2.110088E-11
3.400000E-02	4.210000E+01	9.962368E-12
3.500000E-02	4.210000E+01	4.599542E-12
3.600000E-02	4.210000E+01	2.076588E-12
3.700000E-02	4.210000E+01	9.167807E-13
3.800000E-02	4.210000E+01	3.957820E-13
3.900000E-02	4.210000E+01	1.670781E-13
4.000000E-02	4.210000E+01	6.896892E-14
4.100000E-02	4.210000E+01	2.783917E-14
4.200000E-02	4.210000E+01	1.098821E-14
4.300000E-02	4.210000E+01	4.240956E-15
4.400000E-02	4.210000E+01	1.600540E-15
4.500000E-02	4.210000E+01	5.906554E-16
4.600000E-02	4.210000E+01	2.131407E-16
4.700000E-02	4.210000E+01	7.520778E-17
4.800000E-02	4.210000E+01	2.594913E-17
4.900000E-02	4.210000E+01	8.754804E-18
5.000000E-02	4.210000E+01	2.888240E-18
5.200000E-02	4.210000E+01	2.938975E-19
5.400000E-02	4.210000E+01	2.734070E-20
5.600000E-02	4.210000E+01	2.325272E-21
5.800000E-02	4.210000E+01	1.807956E-22
6.000000E-02	4.210000E+01	1.285143E-23
6.500000E-02	4.210000E+01	1.169367E-26
7.000000E-02	4.210000E+01	6.074444E-30
8.000000E-02	4.210000E+01	3.049900E-37
9.000000E-02	4.210000E+01	1.626642E-45
1.000000E-01	4.210000E+01	6.518515E-52
1.500000E-01	4.210000E+01	1.525200E-112
2.000000E-01	4.210000E+01	1.434647E-197

Pu160000_vs_Z_Vol.log

```
*****
*
*   Deterministic linear equilibrium absorption for pulse injection with   *
*   first-order decay                                                    *
*
*   Pu vs. Depth at R=160,000                                           *
*
*****
```

Model Name = Linear equilibrium
Calculation began 4/6/98 3:52:02 PM

Model parameters:
R = 160000
theta = 0.21
D = 0.53
mu = 0
gamma = 0
q = 0.21
t0 = 0.052
c0 = 0.61

No fit performed; model calculation only

Calculated model curves:

Distance	Time	Model
1.000000E-03	4.210000E+01	9.289142E-06
2.000000E-03	4.210000E+01	9.255815E-06
3.000000E-03	4.210000E+01	9.189054E-06
4.000000E-03	4.210000E+01	9.089609E-06
5.000000E-03	4.210000E+01	8.958584E-06
6.000000E-03	4.210000E+01	8.797415E-06
7.000000E-03	4.210000E+01	8.607846E-06
8.000000E-03	4.210000E+01	8.391888E-06
9.000000E-03	4.210000E+01	8.151781E-06
1.000000E-02	4.210000E+01	7.889952E-06
1.100000E-02	4.210000E+01	7.608980E-06
1.200000E-02	4.210000E+01	7.311552E-06
1.300000E-02	4.210000E+01	7.000424E-06
1.400000E-02	4.210000E+01	6.678380E-06
1.500000E-02	4.210000E+01	6.348194E-06
1.600000E-02	4.210000E+01	6.012594E-06
1.700000E-02	4.210000E+01	5.674223E-06
1.800000E-02	4.210000E+01	5.335611E-06
1.900000E-02	4.210000E+01	4.999142E-06
2.000000E-02	4.210000E+01	4.667033E-06
2.100000E-02	4.210000E+01	4.341311E-06
2.200000E-02	4.210000E+01	4.023799E-06
2.300000E-02	4.210000E+01	3.716103E-06
2.400000E-02	4.210000E+01	3.419605E-06
2.500000E-02	4.210000E+01	3.135464E-06
2.600000E-02	4.210000E+01	2.864615E-06
2.700000E-02	4.210000E+01	2.607773E-06
2.800000E-02	4.210000E+01	2.365449E-06
2.900000E-02	4.210000E+01	2.137953E-06
3.000000E-02	4.210000E+01	1.925414E-06
3.100000E-02	4.210000E+01	1.727795E-06
3.200000E-02	4.210000E+01	1.544909E-06
3.300000E-02	4.210000E+01	1.376436E-06
3.400000E-02	4.210000E+01	1.221946E-06
3.500000E-02	4.210000E+01	1.080914E-06
3.600000E-02	4.210000E+01	9.527358E-07
3.700000E-02	4.210000E+01	8.367507E-07
3.800000E-02	4.210000E+01	7.322529E-07

Pu160000_vs_Z_Vol.log

3.900000E-02	4.210000E+01	6.385087E-07
4.000000E-02	4.210000E+01	5.547687E-07
4.100000E-02	4.210000E+01	4.802809E-07
4.200000E-02	4.210000E+01	4.143003E-07
4.300000E-02	4.210000E+01	3.560984E-07
4.400000E-02	4.210000E+01	3.049702E-07
4.500000E-02	4.210000E+01	2.602408E-07
4.600000E-02	4.210000E+01	2.212694E-07
4.700000E-02	4.210000E+01	1.874530E-07
4.800000E-02	4.210000E+01	1.582289E-07
4.900000E-02	4.210000E+01	1.330755E-07
5.000000E-02	4.210000E+01	1.115131E-07
5.200000E-02	4.210000E+01	7.744845E-08
5.400000E-02	4.210000E+01	5.300474E-08
5.600000E-02	4.210000E+01	3.574341E-08
5.800000E-02	4.210000E+01	2.374749E-08
6.000000E-02	4.210000E+01	1.554309E-08
6.500000E-02	4.210000E+01	5.041761E-09
7.000000E-02	4.210000E+01	1.485540E-09
8.000000E-02	4.210000E+01	1.053218E-10
9.000000E-02	4.210000E+01	5.037118E-12
1.000000E-01	4.210000E+01	1.683228E-13
1.500000E-01	4.210000E+01	3.228899E-23
2.000000E-01	4.210000E+01	7.884676E-37

Pu100000_vs_Z_Vol.log

```
*****
*
*   Deterministic linear equilibrium absorption for pulse injection with   *
*   first-order decay                                                    *
*
*   Pu vs. Depth at R=1,000,000                                         *
*
*****
```

Model Name = Linear equilibrium
Calculation began 4/6/98 3:51:43 PM

Model parameters:
R = 1000000
theta = 0.21
D = 0.53
mu = 0
gamma = 0
q = 0.21
t0 = 0.052
c0 = 0.61

No fit performed; model calculation only

Calculated model curves:

Distance	Time	Model
1.000000E-03	4.210000E+01	3.724750E-06
2.000000E-03	4.210000E+01	3.607561E-06
3.000000E-03	4.210000E+01	3.416109E-06
4.000000E-03	4.210000E+01	3.162857E-06
5.000000E-03	4.210000E+01	2.863340E-06
6.000000E-03	4.210000E+01	2.534592E-06
7.000000E-03	4.210000E+01	2.193681E-06
8.000000E-03	4.210000E+01	1.856362E-06
9.000000E-03	4.210000E+01	1.535960E-06
1.000000E-02	4.210000E+01	1.242625E-06
1.100000E-02	4.210000E+01	9.830223E-07
1.200000E-02	4.210000E+01	7.604526E-07
1.300000E-02	4.210000E+01	5.752850E-07
1.400000E-02	4.210000E+01	4.256010E-07
1.500000E-02	4.210000E+01	3.079094E-07
1.600000E-02	4.210000E+01	2.178303E-07
1.700000E-02	4.210000E+01	1.506757E-07
1.800000E-02	4.210000E+01	1.018900E-07
1.900000E-02	4.210000E+01	6.734350E-08
2.000000E-02	4.210000E+01	4.349380E-08
2.100000E-02	4.210000E+01	2.744086E-08
2.200000E-02	4.210000E+01	1.690664E-08
2.300000E-02	4.210000E+01	1.016803E-08
2.400000E-02	4.210000E+01	5.966840E-09
2.500000E-02	4.210000E+01	3.414801E-09
2.600000E-02	4.210000E+01	1.904836E-09
2.700000E-02	4.210000E+01	1.035012E-09
2.800000E-02	4.210000E+01	5.474076E-10
2.900000E-02	4.210000E+01	3.140107E-10
3.000000E-02	4.210000E+01	1.620821E-10
3.100000E-02	4.210000E+01	8.182148E-11
3.200000E-02	4.210000E+01	4.039453E-11
3.300000E-02	4.210000E+01	1.950233E-11
3.400000E-02	4.210000E+01	9.207643E-12
3.500000E-02	4.210000E+01	4.251092E-12
3.600000E-02	4.210000E+01	1.919271E-12
3.700000E-02	4.210000E+01	8.473276E-13
3.800000E-02	4.210000E+01	3.657985E-13

Pu100000_vs_Z_Vol.log

3.900000E-02	4.210000E+01	1.544206E-13
4.000000E-02	4.210000E+01	6.374400E-14
4.100000E-02	4.210000E+01	2.573014E-14
4.200000E-02	4.210000E+01	1.015577E-14
4.300000E-02	4.210000E+01	3.919671E-15
4.400000E-02	4.210000E+01	1.479287E-15
4.500000E-02	4.210000E+01	5.459088E-16
4.600000E-02	4.210000E+01	1.969937E-16
4.700000E-02	4.210000E+01	6.951022E-17
4.800000E-02	4.210000E+01	2.398329E-17
4.900000E-02	4.210000E+01	8.091561E-18
5.000000E-02	4.210000E+01	2.669434E-18
5.200000E-02	4.210000E+01	2.716325E-19
5.400000E-02	4.210000E+01	2.526943E-20
5.600000E-02	4.210000E+01	2.149115E-21
5.800000E-02	4.210000E+01	1.670990E-22
6.000000E-02	4.210000E+01	1.187784E-23
6.500000E-02	4.210000E+01	1.080779E-26
7.000000E-02	4.210000E+01	5.614259E-30
8.000000E-02	4.210000E+01	2.818847E-37
9.000000E-02	4.210000E+01	1.503412E-45
1.000000E-01	4.210000E+01	6.024688E-52
1.500000E-01	4.210000E+01	1.409654E-112
2.000000E-01	4.210000E+01	1.325962E-197

APPENDIX I

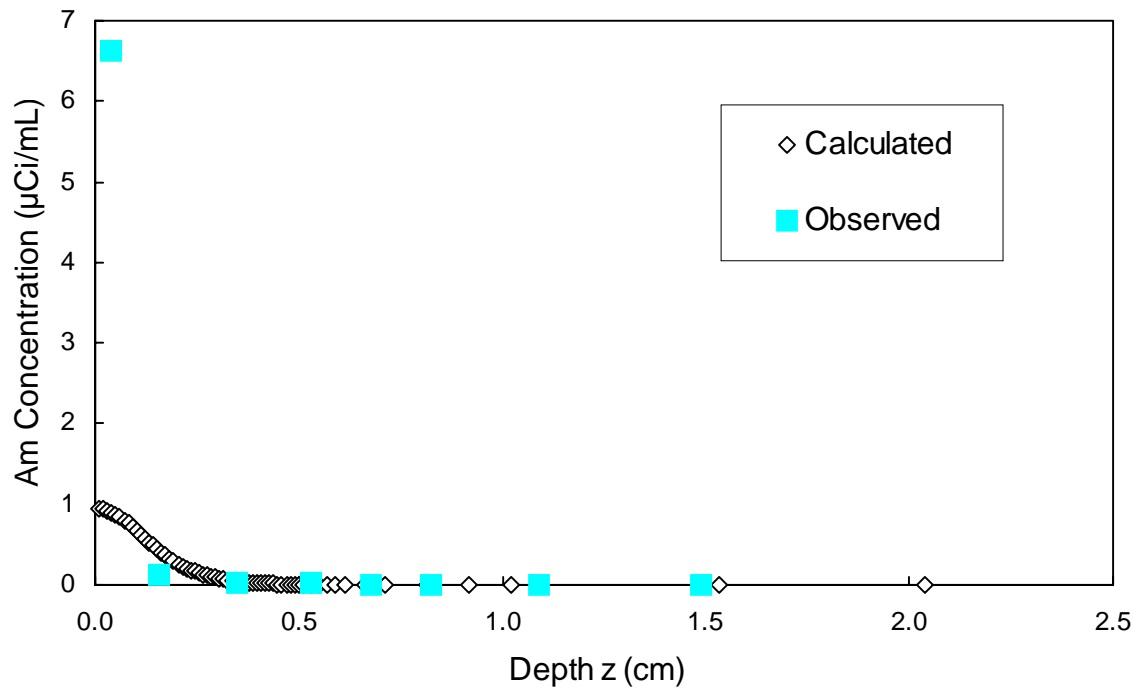
**LISTINGS OF EXCEL 97 SPREADSHEETS SHOWING CALCULATED VS.
OBSERVED ACTINIDE CONCENTRATION AS FUNCTION OF DEPTH**

Am-241 Calculated vs. Observed for R = 160,000

R =	Theta =	Total Am			
160000.0	0.21	Concentration			
Length (z/L)	Pore Volumes	Dissolved Am Concentration (μCi/mL)	Depth Z (cm)	Calculated	Observed
0.001	42.1	2.82E-05	0.010	9.46E-01	
0.002	42.1	2.79E-05	0.020	9.38E-01	
0.003	42.1	2.74E-05	0.031	9.22E-01	
			0.037		6.63E-00
0.004	42.1	2.68E-05	0.041	8.99E-01	
0.005	42.1	2.59E-05	0.051	8.71E-01	
0.006	42.1	2.49E-05	0.061	8.38E-01	
0.007	42.1	2.38E-05	0.071	8.00E-01	
0.008	42.1	2.26E-05	0.082	7.59E-01	
0.009	42.1	2.13E-05	0.092	7.15E-01	
0.010	42.1	1.99E-05	0.102	6.69E-01	
0.011	42.1	1.85E-05	0.112	6.23E-01	
0.012	42.1	1.71E-05	0.122	5.76E-01	
0.013	42.1	1.58E-05	0.133	5.29E-01	
0.014	42.1	1.44E-05	0.143	4.84E-01	
0.015	42.1	1.31E-05	0.153	4.41E-01	
			0.159		1.17E-01
0.016	42.1	1.19E-05	0.163	4.00E-01	
0.017	42.1	1.07E-05	0.173	3.61E-01	
0.018	42.1	9.67E-06	0.184	3.25E-01	
0.019	42.1	8.67E-06	0.194	2.91E-01	
0.020	42.1	7.75E-06	0.204	2.60E-01	
0.021	42.1	6.92E-06	0.214	2.32E-01	
0.022	42.1	6.16E-06	0.224	2.07E-01	
0.023	42.1	5.47E-06	0.235	1.84E-01	
0.024	42.1	4.86E-06	0.245	1.63E-01	
0.025	42.1	4.31E-06	0.255	1.45E-01	
0.026	42.1	3.82E-06	0.265	1.28E-01	
0.027	42.1	3.38E-06	0.275	1.13E-01	
0.028	42.1	2.99E-06	0.286	1.00E-01	
0.029	42.1	2.64E-06	0.296	8.86E-02	
0.030	42.1	2.33E-06	0.306	7.82E-02	
0.031	42.1	2.05E-06	0.316	6.89E-02	
0.032	42.1	1.81E-06	0.326	6.07E-02	
0.033	42.1	1.59E-06	0.337	5.33E-02	
0.034	42.1	1.39E-06	0.347	4.68E-02	
			0.351		1.30E-02
0.035	42.1	1.22E-06	0.357	4.10E-02	
0.036	42.1	1.07E-06	0.367	3.58E-02	
0.037	42.1	9.30E-07	0.377	3.13E-02	
0.038	42.1	8.10E-07	0.388	2.72E-02	
0.039	42.1	7.03E-07	0.398	2.36E-02	
0.040	42.1	6.08E-07	0.408	2.04E-02	
0.041	42.1	5.25E-07	0.418	1.76E-02	
0.042	42.1	4.52E-07	0.428	1.52E-02	
0.043	42.1	3.88E-07	0.439	1.30E-02	

Am-241 Calculated vs. Observed for R = 160,000

0.044	42.1	3.32E-07	0.449	1.11E-02	
0.045	42.1	2.83E-07	0.459	9.50E-03	
0.046	42.1	2.40E-07	0.469	8.07E-03	
0.047	42.1	2.03E-07	0.479	6.83E-03	
0.048	42.1	1.71E-07	0.490	5.76E-03	
0.049	42.1	1.44E-07	0.500	4.84E-03	
0.050	42.1	1.21E-07	0.510	4.06E-03	
0.052	42.1	8.38E-08	0.530	2.82E-03	
			0.531		1.30E-02
0.054	42.1	5.74E-08	0.551	1.93E-03	
0.056	42.1	3.87E-08	0.571	1.30E-03	
0.058	42.1	2.57E-08	0.592	8.63E-04	
0.060	42.1	1.68E-08	0.612	5.65E-04	
0.065	42.1	5.46E-09	0.663	1.83E-04	
			0.679		8.30E-04
0.070	42.1	1.61E-09	0.714	5.40E-05	
0.080	42.1	1.14E-10	0.816	3.83E-06	
			0.826		5.20E-04
0.090	42.1	5.45E-12	0.918	1.83E-07	
0.100	42.1	1.82E-13	1.020	6.12E-09	
			1.088		2.20E-04
			1.487		1.80E-04
0.150	42.1	3.49E-23	1.530	1.17E-18	
0.200	42.1	8.53E-37	2.040	2.87E-32	



AM-241 Calculated vs. Observed for R = 160,000

R = Length (z/L)	160000 Pore Volumes	Dissolved Am Concentration ($\mu\text{Ci/mL}$)	Theta = 0.21 Depth Z (cm)	Total Am Concentration ($\mu\text{Ci/mL}$) Calculated	Observed
0.001	42.1	0.00002816805	=10.2*A5	=\$B\$1*\$D\$1*C5	
0.002	42.1	0.00002790231	=10.2*A6	=\$B\$1*\$D\$1*C6	
0.003	42.1	0.00002743187	=10.2*A7	=\$B\$1*\$D\$1*C7	
			0.037		6.63
0.004	42.1	0.00002676909	=10.2*A9	=\$B\$1*\$D\$1*C9	
0.005	42.1	0.00002593103	=10.2*A10	=\$B\$1*\$D\$1*C10	
0.006	42.1	0.00002493851	=10.2*A11	=\$B\$1*\$D\$1*C11	
0.007	42.1	0.00002381512	=10.2*A12	=\$B\$1*\$D\$1*C12	
0.008	42.1	0.00002258624	=10.2*A13	=\$B\$1*\$D\$1*C13	
0.009	42.1	0.00002127811	=10.2*A14	=\$B\$1*\$D\$1*C14	
0.01	42.1	0.00001991689	=10.2*A15	=\$B\$1*\$D\$1*C15	
0.011	42.1	0.00001852784	=10.2*A16	=\$B\$1*\$D\$1*C16	
0.012	42.1	0.0000171345	=10.2*A17	=\$B\$1*\$D\$1*C17	
0.013	42.1	0.00001575811	=10.2*A18	=\$B\$1*\$D\$1*C18	
0.014	42.1	0.00001441707	=10.2*A19	=\$B\$1*\$D\$1*C19	
0.015	42.1	0.00001312671	=10.2*A20	=\$B\$1*\$D\$1*C20	
			0.159		0.117
0.016	42.1	0.00001189914	=10.2*A22	=\$B\$1*\$D\$1*C22	
0.017	42.1	0.00001074328	=10.2*A23	=\$B\$1*\$D\$1*C23	
0.018	42.1	0.00000966505	=10.2*A24	=\$B\$1*\$D\$1*C24	
0.019	42.1	0.000008667623	=10.2*A25	=\$B\$1*\$D\$1*C25	
0.02	42.1	0.000007751812	=10.2*A26	=\$B\$1*\$D\$1*C26	
0.021	42.1	0.000006916449	=10.2*A27	=\$B\$1*\$D\$1*C27	
0.022	42.1	0.000006158793	=10.2*A28	=\$B\$1*\$D\$1*C28	
0.023	42.1	0.000005474934	=10.2*A29	=\$B\$1*\$D\$1*C29	
0.024	42.1	0.000004860155	=10.2*A30	=\$B\$1*\$D\$1*C30	
0.025	42.1	0.000004309257	=10.2*A31	=\$B\$1*\$D\$1*C31	
0.026	42.1	0.000003816832	=10.2*A32	=\$B\$1*\$D\$1*C32	
0.027	42.1	0.000003377484	=10.2*A33	=\$B\$1*\$D\$1*C33	
0.028	42.1	0.000002985988	=10.2*A34	=\$B\$1*\$D\$1*C34	
0.029	42.1	0.000002637413	=10.2*A35	=\$B\$1*\$D\$1*C35	
0.03	42.1	0.000002327195	=10.2*A36	=\$B\$1*\$D\$1*C36	
0.031	42.1	0.000002051175	=10.2*A37	=\$B\$1*\$D\$1*C37	
0.032	42.1	0.00000180561	=10.2*A38	=\$B\$1*\$D\$1*C38	
0.033	42.1	0.000001587163	=10.2*A39	=\$B\$1*\$D\$1*C39	
0.034	42.1	0.000001392881	=10.2*A40	=\$B\$1*\$D\$1*C40	
			0.351		0.013
0.035	42.1	0.000001220158	=10.2*A42	=\$B\$1*\$D\$1*C42	
0.036	42.1	0.000001066698	=10.2*A43	=\$B\$1*\$D\$1*C43	
0.037	42.1	0.0000009304788	=10.2*A44	=\$B\$1*\$D\$1*C44	
0.038	42.1	0.0000008097132	=10.2*A45	=\$B\$1*\$D\$1*C45	
0.039	42.1	0.000000702815	=10.2*A46	=\$B\$1*\$D\$1*C46	
0.04	42.1	0.0000006083696	=10.2*A47	=\$B\$1*\$D\$1*C47	
0.041	42.1	0.0000005251083	=10.2*A48	=\$B\$1*\$D\$1*C48	
0.042	42.1	0.0000004518874	=10.2*A49	=\$B\$1*\$D\$1*C49	
0.043	42.1	0.0000003876709	=10.2*A50	=\$B\$1*\$D\$1*C50	
0.044	42.1	0.0000003316303	=10.2*A51	=\$B\$1*\$D\$1*C51	
0.045	42.1	0.0000002826542	=10.2*A52	=\$B\$1*\$D\$1*C52	
0.046	42.1	0.0000002401038	=10.2*A53	=\$B\$1*\$D\$1*C53	
0.047	42.1	0.0000002032634	=10.2*A54	=\$B\$1*\$D\$1*C54	
0.048	42.1	0.0000001714801	=10.2*A55	=\$B\$1*\$D\$1*C55	
0.049	42.1	0.0000001441597	=10.2*A56	=\$B\$1*\$D\$1*C56	
0.05	42.1	0.0000001207629	=10.2*A57	=\$B\$1*\$D\$1*C57	
0.052	42.1	0.0000000838376	=10.2*A58	=\$B\$1*\$D\$1*C58	

AM-241 Calculated vs. Observed for R = 160,000

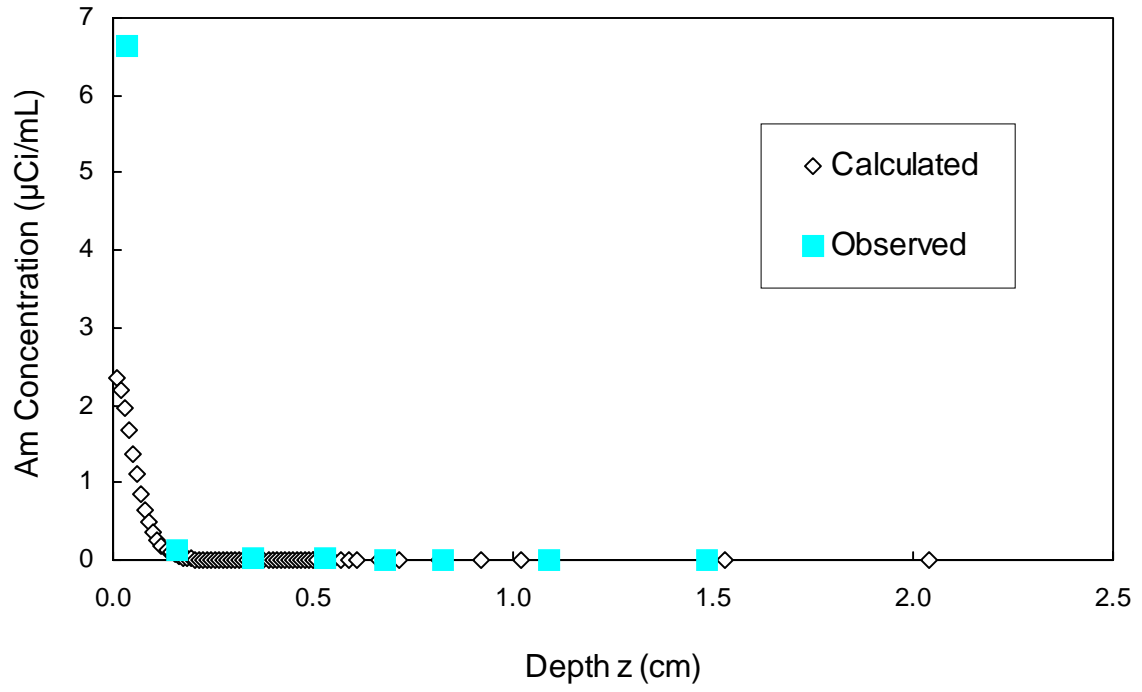
0.054	42.1	0.00000005736411	=10.2*A60	=\$B\$1*\$D\$1*C60	
0.056	42.1	0.00000003867829	=10.2*A61	=\$B\$1*\$D\$1*C61	
0.058	42.1	0.0000000256957	=10.2*A62	=\$B\$1*\$D\$1*C62	
0.06	42.1	0.00000001681766	=10.2*A63	=\$B\$1*\$D\$1*C63	
0.065	42.1	0.000000005455047	=10.2*A64	=\$B\$1*\$D\$1*C64	
			0.679		0.00083
0.07	42.1	0.000000001607306	=10.2*A66	=\$B\$1*\$D\$1*C66	
0.08	42.1	0.0000000001139548	=10.2*A67	=\$B\$1*\$D\$1*C67	
			0.826		0.00052
0.09	42.1	0.000000000005449997	=10.2*A69	=\$B\$1*\$D\$1*C69	
0.1	42.1	0.0000000000001821197	=10.2*A70	=\$B\$1*\$D\$1*C70	
			1.088		0.00022
			1.487		0.00018
0.15	42.1	3.493562E-23	=10.2*A73	=\$B\$1*\$D\$1*C73	
0.2	42.1	8.530961E-37	=10.2*A74	=\$B\$1*\$D\$1*C74	

AM-241 Calculated vs. Observed for R = 1,000,000

R =	Theta =	Total Am			
1000000.0	0.21	Concentration			
Length (z/L)	Pore Volumes	Dissolved Am Concentration (μCi/mL)	Depth Z (cm)	Calculated	Observed
0.001	42.1	1.11E-05	0.010	2.34E-00	
0.002	42.1	1.04E-05	0.020	2.19E-00	
0.003	42.1	9.30E-06	0.031	1.95E-00	
			0.037		6.63E-00
0.004	42.1	7.97E-06	0.041	1.67E-00	
0.005	42.1	6.56E-06	0.051	1.38E-00	
0.006	42.1	5.23E-06	0.061	1.10E-00	
0.007	42.1	4.06E-06	0.071	8.52E-01	
0.008	42.1	3.08E-06	0.082	6.47E-01	
0.009	42.1	2.30E-06	0.092	4.84E-01	
0.010	42.1	1.71E-06	0.102	3.59E-01	
0.011	42.1	1.26E-06	0.112	2.64E-01	
0.012	42.1	9.19E-07	0.122	1.93E-01	
0.013	42.1	6.67E-07	0.133	1.40E-01	
0.014	42.1	4.80E-07	0.143	1.01E-01	
0.015	42.1	3.41E-07	0.153	7.17E-02	
			0.159		1.17E-01
0.016	42.1	2.39E-07	0.163	5.01E-02	
0.017	42.1	1.64E-07	0.173	3.45E-02	
0.018	42.1	1.11E-07	0.184	2.32E-02	
0.019	42.1	7.30E-08	0.194	1.53E-02	
0.020	42.1	4.71E-08	0.204	9.89E-03	
0.021	42.1	2.97E-08	0.214	6.24E-03	
0.022	42.1	1.83E-08	0.224	3.84E-03	
0.023	42.1	1.10E-08	0.235	2.31E-03	
0.024	42.1	6.46E-09	0.245	1.36E-03	
0.025	42.1	3.69E-09	0.255	7.76E-04	
0.026	42.1	2.06E-09	0.265	4.33E-04	
0.027	42.1	1.12E-09	0.275	2.35E-04	
0.028	42.1	5.92E-10	0.286	1.24E-04	
0.029	42.1	3.40E-10	0.296	7.13E-05	
0.030	42.1	1.75E-10	0.306	3.68E-05	
0.031	42.1	8.85E-11	0.316	1.86E-05	
0.032	42.1	4.37E-11	0.326	9.18E-06	
0.033	42.1	2.11E-11	0.337	4.43E-06	
0.034	42.1	9.96E-12	0.347	2.09E-06	
			0.351		1.30E-02
0.035	42.1	4.60E-12	0.357	9.66E-07	
0.036	42.1	2.08E-12	0.367	4.36E-07	
0.037	42.1	9.17E-13	0.377	1.93E-07	
0.038	42.1	3.96E-13	0.388	8.31E-08	
0.039	42.1	1.67E-13	0.398	3.51E-08	
0.040	42.1	6.90E-14	0.408	1.45E-08	
0.041	42.1	2.78E-14	0.418	5.85E-09	
0.042	42.1	1.10E-14	0.428	2.31E-09	
0.043	42.1	4.24E-15	0.439	8.91E-10	
0.044	42.1	1.60E-15	0.449	3.36E-10	
0.045	42.1	5.91E-16	0.459	1.24E-10	
0.046	42.1	2.13E-16	0.469	4.48E-11	
0.047	42.1	7.52E-17	0.479	1.58E-11	

AM-241 Calculated vs. Observed for R = 1,000,000

0.048	42.1	2.59E-17	0.490	5.45E-12	
0.049	42.1	8.75E-18	0.500	1.84E-12	
0.050	42.1	2.89E-18	0.510	6.07E-13	
0.052	42.1	2.94E-19	0.530	6.17E-14	
			0.531		1.30E-02
0.054	42.1	2.73E-20	0.551	5.74E-15	
0.056	42.1	2.33E-21	0.571	4.88E-16	
0.058	42.1	1.81E-22	0.592	3.80E-17	
0.060	42.1	1.29E-23	0.612	2.70E-18	
0.065	42.1	1.17E-26	0.663	2.46E-21	
			0.679		8.30E-04
0.070	42.1	6.07E-30	0.714	1.28E-24	
0.080	42.1	3.05E-37	0.816	6.40E-32	
			0.826		5.20E-04
0.090	42.1	1.63E-45	0.918	3.42E-40	
0.100	42.1	6.52E-52	1.020	1.37E-46	
			1.088		2.20E-04
			1.487		1.80E-04
0.150	42.1	1.53E-11	1.530	3.20E-06	
0.200	42.1	1.43E-19	2.040	3.01E-14	



Am-241 Calculated vs Observed for R = 1,000,000

R =	1000000		Theta =	0.21		Total Am	
Length	Pore	Dissolved Am			Depth Z (cm)	Concentration	
(z/L)	Volumes	Concentration				($\mu\text{Ci/mL}$)	Observed
		($\mu\text{Ci/mL}$)				Calculated	
0.001	42.1	0.00001114651			=10.2*A5	=B\$1*\$D\$1*C5	
0.002	42.1	0.00001041313			=10.2*A6	=B\$1*\$D\$1*C6	
0.003	42.1	0.000009301828			=10.2*A7	=B\$1*\$D\$1*C7	
					0.037		6.63
0.004	42.1	0.000007966166			=10.2*A9	=B\$1*\$D\$1*C9	
0.005	42.1	0.000006564837			=10.2*A10	=B\$1*\$D\$1*C10	
0.006	42.1	0.000005231721			=10.2*A11	=B\$1*\$D\$1*C11	
0.007	42.1	0.000004056345			=10.2*A12	=B\$1*\$D\$1*C12	
0.008	42.1	0.00000307988			=10.2*A13	=B\$1*\$D\$1*C13	
0.009	42.1	0.00000230426			=10.2*A14	=B\$1*\$D\$1*C14	
0.01	42.1	0.000001707177			=10.2*A15	=B\$1*\$D\$1*C15	
0.011	42.1	0.000001256265			=10.2*A16	=B\$1*\$D\$1*C16	
0.012	42.1	0.0000009189481			=10.2*A17	=B\$1*\$D\$1*C17	
0.013	42.1	0.0000006674512			=10.2*A18	=B\$1*\$D\$1*C18	
0.014	42.1	0.0000004801959			=10.2*A19	=B\$1*\$D\$1*C19	
0.015	42.1	0.0000003411962			=10.2*A20	=B\$1*\$D\$1*C20	
					0.159		0.117
0.016	42.1	0.0000002387381			=10.2*A22	=B\$1*\$D\$1*C22	
0.017	42.1	0.0000001640962			=10.2*A23	=B\$1*\$D\$1*C23	
0.018	42.1	0.0000001106656			=10.2*A24	=B\$1*\$D\$1*C24	
0.019	42.1	0.00000007300206			=10.2*A25	=B\$1*\$D\$1*C25	
0.02	42.1	0.00000004710155			=10.2*A26	=B\$1*\$D\$1*C26	
0.021	42.1	0.00000002970249			=10.2*A27	=B\$1*\$D\$1*C27	
0.022	42.1	0.00000001829581			=10.2*A28	=B\$1*\$D\$1*C28	
0.023	42.1	0.00000001100234			=10.2*A29	=B\$1*\$D\$1*C29	
0.024	42.1	0.000000006456136			=10.2*A30	=B\$1*\$D\$1*C30	
0.025	42.1	0.000000003694751			=10.2*A31	=B\$1*\$D\$1*C31	
0.026	42.1	0.00000000206098			=10.2*A32	=B\$1*\$D\$1*C32	
0.027	42.1	0.000000001119851			=10.2*A33	=B\$1*\$D\$1*C33	
0.028	42.1	0.0000000005922775			=10.2*A34	=B\$1*\$D\$1*C34	
0.029	42.1	0.0000000003397494			=10.2*A35	=B\$1*\$D\$1*C35	
0.03	42.1	0.0000000001753675			=10.2*A36	=B\$1*\$D\$1*C36	
0.031	42.1	0.00000000008852817			=10.2*A37	=B\$1*\$D\$1*C37	
0.032	42.1	0.00000000004370556			=10.2*A38	=B\$1*\$D\$1*C38	
0.033	42.1	0.00000000002110088			=10.2*A39	=B\$1*\$D\$1*C39	
0.034	42.1	0.000000000009962368			=10.2*A40	=B\$1*\$D\$1*C40	
					0.351		0.013
0.035	42.1	0.000000000004599542			=10.2*A42	=B\$1*\$D\$1*C42	
0.036	42.1	0.000000000002076588			=10.2*A43	=B\$1*\$D\$1*C43	
0.037	42.1	0.0000000000009167807			=10.2*A44	=B\$1*\$D\$1*C44	
0.038	42.1	0.000000000000395782			=10.2*A45	=B\$1*\$D\$1*C45	
0.039	42.1	0.0000000000001670781			=10.2*A46	=B\$1*\$D\$1*C46	
0.04	42.1	6.896892E-14			=10.2*A47	=B\$1*\$D\$1*C47	
0.041	42.1	2.783917E-14			=10.2*A48	=B\$1*\$D\$1*C48	
0.042	42.1	1.098821E-14			=10.2*A49	=B\$1*\$D\$1*C49	
0.043	42.1	4.240956E-15			=10.2*A50	=B\$1*\$D\$1*C50	
0.044	42.1	1.60054E-15			=10.2*A51	=B\$1*\$D\$1*C51	
0.045	42.1	5.906554E-16			=10.2*A52	=B\$1*\$D\$1*C52	

Am-241 Calculated vs Observed for R = 1,000,000

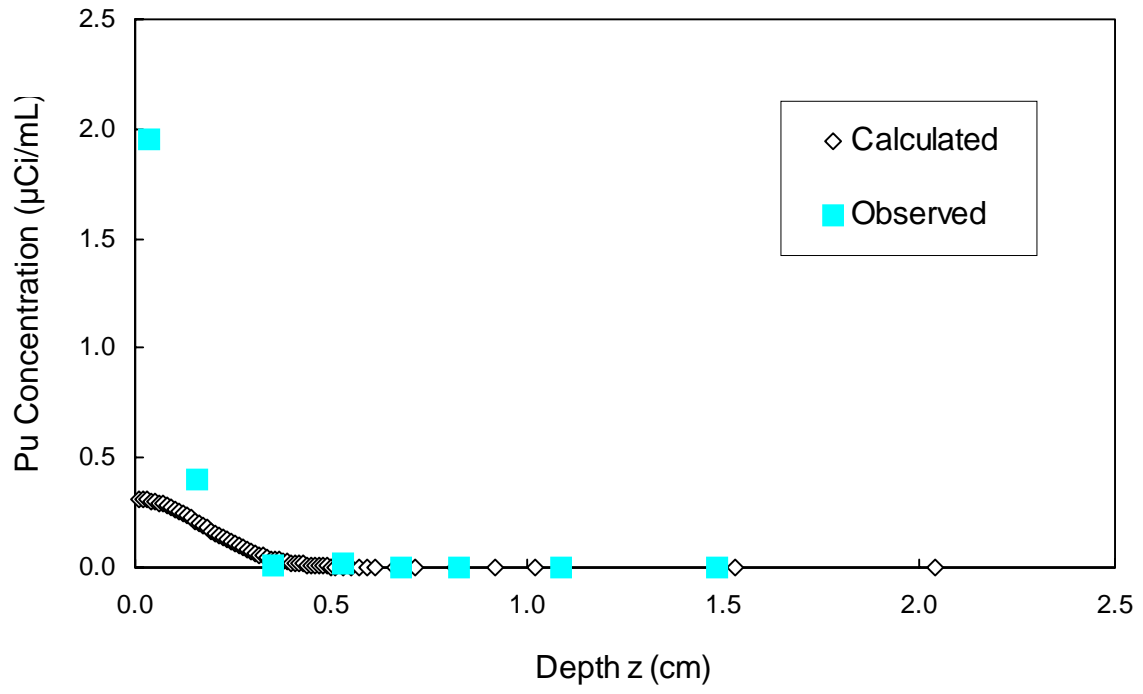
0.046	42.1	2.131407E-16	=10.2*A53	=\$B\$1*\$D\$1*C53	
0.047	42.1	7.520778E-17	=10.2*A54	=\$B\$1*\$D\$1*C54	
0.048	42.1	2.594913E-17	=10.2*A55	=\$B\$1*\$D\$1*C55	
0.049	42.1	8.754804E-18	=10.2*A56	=\$B\$1*\$D\$1*C56	
0.05	42.1	2.88824E-18	=10.2*A57	=\$B\$1*\$D\$1*C57	
0.052	42.1	2.938975E-19	=10.2*A58	=\$B\$1*\$D\$1*C58	
			0.531		0.013
0.054	42.1	2.73407E-20	=10.2*A60	=\$B\$1*\$D\$1*C60	
0.056	42.1	2.325272E-21	=10.2*A61	=\$B\$1*\$D\$1*C61	
0.058	42.1	1.807956E-22	=10.2*A62	=\$B\$1*\$D\$1*C62	
0.06	42.1	1.285143E-23	=10.2*A63	=\$B\$1*\$D\$1*C63	
0.065	42.1	1.169367E-26	=10.2*A64	=\$B\$1*\$D\$1*C64	
			0.679		0.00083
0.07	42.1	6.074444E-30	=10.2*A66	=\$B\$1*\$D\$1*C66	
0.08	42.1	3.0499E-37	=10.2*A67	=\$B\$1*\$D\$1*C67	
			0.826		0.00052
0.09	42.1	1.626642E-45	=10.2*A69	=\$B\$1*\$D\$1*C69	
0.1	42.1	6.518515E-52	=10.2*A70	=\$B\$1*\$D\$1*C70	
			1.088		0.00022
			1.487		0.00018
0.15	42.1	0.000000000015252	=10.2*A73	=\$B\$1*\$D\$1*C73	
0.2	42.1	1.434647E-19	=10.2*A74	=\$B\$1*\$D\$1*C74	

Pu-241 Calculated vs Observed for R = 160,000

R = 160000.0		Theta = 0.21		Total Pu	
Length (z/L)	Pore Volumes	Dissolved Pu Concentration (μCi/mL)	Depth Z (cm)	Concentration (μCi/mL)	Observed
				Calculated	
0.001	42.1	9.29E-06	0.010	3.12E-01	
0.002	42.1	9.26E-06	0.020	3.11E-01	
0.003	42.1	9.19E-06	0.031	3.09E-01	
			0.037		1.95E+00
0.004	42.1	9.09E-06	0.041	3.05E-01	
0.005	42.1	8.96E-06	0.051	3.01E-01	
0.006	42.1	8.80E-06	0.061	2.96E-01	
0.007	42.1	8.61E-06	0.071	2.89E-01	
0.008	42.1	8.39E-06	0.082	2.82E-01	
0.009	42.1	8.15E-06	0.092	2.74E-01	
0.010	42.1	7.89E-06	0.102	2.65E-01	
0.011	42.1	7.61E-06	0.112	2.56E-01	
0.012	42.1	7.31E-06	0.122	2.46E-01	
0.013	42.1	7.00E-06	0.133	2.35E-01	
0.014	42.1	6.68E-06	0.143	2.24E-01	
0.015	42.1	6.35E-06	0.153	2.13E-01	
			0.159		4.00E-01
0.016	42.1	6.01E-06	0.163	2.02E-01	
0.017	42.1	5.67E-06	0.173	1.91E-01	
0.018	42.1	5.34E-06	0.184	1.79E-01	
0.019	42.1	5.00E-06	0.194	1.68E-01	
0.020	42.1	4.67E-06	0.204	1.57E-01	
0.021	42.1	4.34E-06	0.214	1.46E-01	
0.022	42.1	4.02E-06	0.224	1.35E-01	
0.023	42.1	3.72E-06	0.235	1.25E-01	
0.024	42.1	3.42E-06	0.245	1.15E-01	
0.025	42.1	3.14E-06	0.255	1.05E-01	
0.026	42.1	2.86E-06	0.265	9.63E-02	
0.027	42.1	2.61E-06	0.275	8.76E-02	
0.028	42.1	2.37E-06	0.286	7.95E-02	
0.029	42.1	2.14E-06	0.296	7.18E-02	
0.030	42.1	1.93E-06	0.306	6.47E-02	
0.031	42.1	1.73E-06	0.316	5.81E-02	
0.032	42.1	1.54E-06	0.326	5.19E-02	
0.033	42.1	1.38E-06	0.337	4.62E-02	
0.034	42.1	1.22E-06	0.347	4.11E-02	
			0.351		1.02E-02
0.035	42.1	1.08E-06	0.357	3.63E-02	
0.036	42.1	9.53E-07	0.367	3.20E-02	
0.037	42.1	8.37E-07	0.377	2.81E-02	
0.038	42.1	7.32E-07	0.388	2.46E-02	
0.039	42.1	6.39E-07	0.398	2.15E-02	
0.040	42.1	5.55E-07	0.408	1.86E-02	
0.041	42.1	4.80E-07	0.418	1.61E-02	
0.042	42.1	4.14E-07	0.428	1.39E-02	
0.043	42.1	3.56E-07	0.439	1.20E-02	

Pu-241 Calculated vs Observed for R = 160,000

0.044	42.1	3.05E-07	0.449	1.02E-02	
0.045	42.1	2.60E-07	0.459	8.74E-03	
0.046	42.1	2.21E-07	0.469	7.43E-03	
0.047	42.1	1.87E-07	0.479	6.30E-03	
0.048	42.1	1.58E-07	0.490	5.32E-03	
0.049	42.1	1.33E-07	0.500	4.47E-03	
0.050	42.1	1.12E-07	0.510	3.75E-03	
0.052	42.1	7.74E-08	0.530	2.60E-03	
			0.531		1.69E-02
0.054	42.1	5.30E-08	0.551	1.78E-03	
0.056	42.1	3.57E-08	0.571	1.20E-03	
0.058	42.1	2.37E-08	0.592	7.98E-04	
0.060	42.1	1.55E-08	0.612	5.22E-04	
0.065	42.1	5.04E-09	0.663	1.69E-04	
			0.679		7.75E-05
0.070	42.1	1.49E-09	0.714	4.99E-05	
0.080	42.1	1.05E-10	0.816	3.54E-06	
			0.826		4.10E-05
0.090	42.1	5.04E-12	0.918	1.69E-07	
0.100	42.1	1.68E-13	1.020	5.66E-09	
			1.088		3.94E-05
			1.487		3.86E-05
0.150	42.1	3.23E-23	1.530	1.08E-18	
0.200	42.1	7.88E-37	2.040	2.65E-32	



Pu-241 Calculated vs. Observed for R=160,000

R =	160000	Theta =	0.21	Total Pu	
Length	Pore	Dissolved Pu		Concentration	
(z/L)	Volumes	Concentration	Depth Z (cm)	($\mu\text{Ci/mL}$)	Observed
		($\mu\text{Ci/mL}$)		Calculated	
0.001	42.1	0.000009289142	=10.2*A5	=B\$1*\$D\$1*C5	
0.002	42.1	0.000009255815	=10.2*A6	=B\$1*\$D\$1*C6	
0.003	42.1	0.000009189054	=10.2*A7	=B\$1*\$D\$1*C7	
			0.037		1.95
0.004	42.1	0.000009089609	=10.2*A9	=B\$1*\$D\$1*C9	
0.005	42.1	0.000008958584	=10.2*A10	=B\$1*\$D\$1*C10	
0.006	42.1	0.000008797415	=10.2*A11	=B\$1*\$D\$1*C11	
0.007	42.1	0.000008607846	=10.2*A12	=B\$1*\$D\$1*C12	
0.008	42.1	0.000008391888	=10.2*A13	=B\$1*\$D\$1*C13	
0.009	42.1	0.000008151781	=10.2*A14	=B\$1*\$D\$1*C14	
0.01	42.1	0.000007889952	=10.2*A15	=B\$1*\$D\$1*C15	
0.011	42.1	0.00000760898	=10.2*A16	=B\$1*\$D\$1*C16	
0.012	42.1	0.000007311552	=10.2*A17	=B\$1*\$D\$1*C17	
0.013	42.1	0.000007000424	=10.2*A18	=B\$1*\$D\$1*C18	
0.014	42.1	0.00000667838	=10.2*A19	=B\$1*\$D\$1*C19	
0.015	42.1	0.000006348194	=10.2*A20	=B\$1*\$D\$1*C20	
			0.159		0.4
0.016	42.1	0.000006012594	=10.2*A22	=B\$1*\$D\$1*C22	
0.017	42.1	0.000005674223	=10.2*A23	=B\$1*\$D\$1*C23	
0.018	42.1	0.000005335611	=10.2*A24	=B\$1*\$D\$1*C24	
0.019	42.1	0.000004999142	=10.2*A25	=B\$1*\$D\$1*C25	
0.02	42.1	0.000004667033	=10.2*A26	=B\$1*\$D\$1*C26	
0.021	42.1	0.000004341311	=10.2*A27	=B\$1*\$D\$1*C27	
0.022	42.1	0.000004023799	=10.2*A28	=B\$1*\$D\$1*C28	
0.023	42.1	0.000003716103	=10.2*A29	=B\$1*\$D\$1*C29	
0.024	42.1	0.000003419605	=10.2*A30	=B\$1*\$D\$1*C30	
0.025	42.1	0.000003135464	=10.2*A31	=B\$1*\$D\$1*C31	
0.026	42.1	0.000002864615	=10.2*A32	=B\$1*\$D\$1*C32	
0.027	42.1	0.000002607773	=10.2*A33	=B\$1*\$D\$1*C33	
0.028	42.1	0.000002365449	=10.2*A34	=B\$1*\$D\$1*C34	
0.029	42.1	0.000002137953	=10.2*A35	=B\$1*\$D\$1*C35	
0.03	42.1	0.000001925414	=10.2*A36	=B\$1*\$D\$1*C36	
0.031	42.1	0.000001727795	=10.2*A37	=B\$1*\$D\$1*C37	
0.032	42.1	0.000001544909	=10.2*A38	=B\$1*\$D\$1*C38	
0.033	42.1	0.000001376436	=10.2*A39	=B\$1*\$D\$1*C39	
0.034	42.1	0.000001221946	=10.2*A40	=B\$1*\$D\$1*C40	
			0.351		0.0102
0.035	42.1	0.000001080914	=10.2*A42	=B\$1*\$D\$1*C42	
0.036	42.1	0.0000009527358	=10.2*A43	=B\$1*\$D\$1*C43	
0.037	42.1	0.0000008367507	=10.2*A44	=B\$1*\$D\$1*C44	
0.038	42.1	0.0000007322529	=10.2*A45	=B\$1*\$D\$1*C45	
0.039	42.1	0.0000006385087	=10.2*A46	=B\$1*\$D\$1*C46	
0.04	42.1	0.0000005547687	=10.2*A47	=B\$1*\$D\$1*C47	
0.041	42.1	0.0000004802809	=10.2*A48	=B\$1*\$D\$1*C48	
0.042	42.1	0.0000004143003	=10.2*A49	=B\$1*\$D\$1*C49	
0.043	42.1	0.0000003560984	=10.2*A50	=B\$1*\$D\$1*C50	
0.044	42.1	0.0000003049702	=10.2*A51	=B\$1*\$D\$1*C51	
0.045	42.1	0.0000002602408	=10.2*A52	=B\$1*\$D\$1*C52	

Pu-241 Calculated vs. Observed for R=160,000

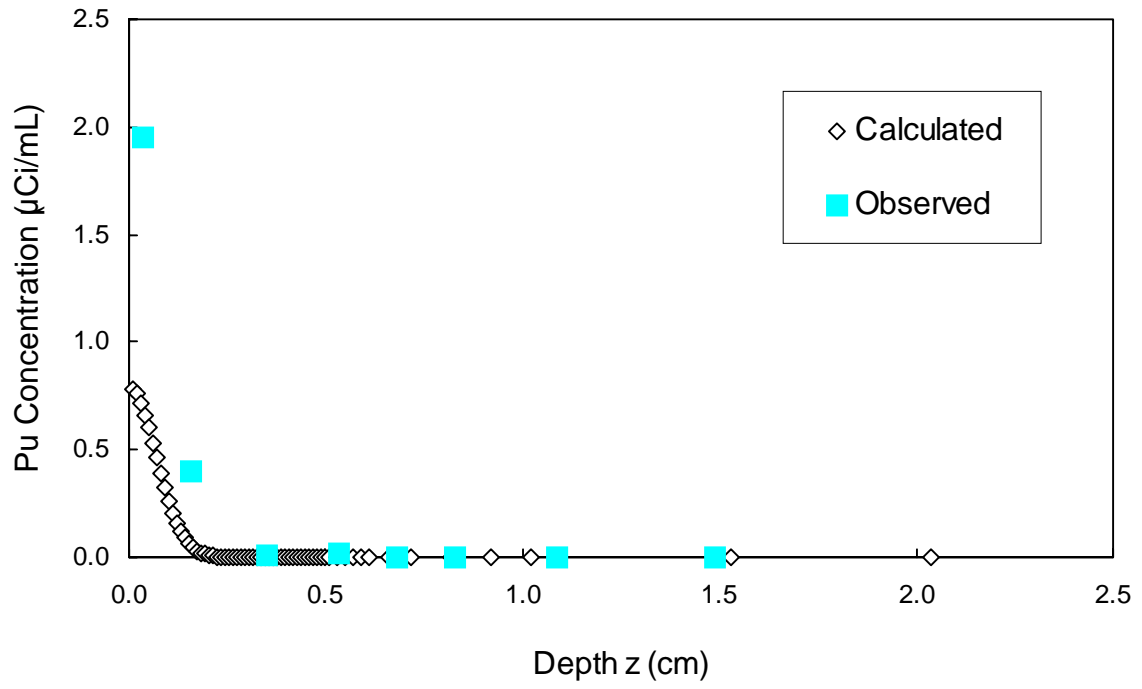
0.046	42.1	0.0000002212694	=10.2*A53	=\$B\$1*\$D\$1*C53	
0.047	42.1	0.000000187453	=10.2*A54	=\$B\$1*\$D\$1*C54	
0.048	42.1	0.0000001582289	=10.2*A55	=\$B\$1*\$D\$1*C55	
0.049	42.1	0.0000001330755	=10.2*A56	=\$B\$1*\$D\$1*C56	
0.05	42.1	0.0000001115131	=10.2*A57	=\$B\$1*\$D\$1*C57	
0.052	42.1	0.00000007744845	=10.2*A58	=\$B\$1*\$D\$1*C58	
			0.531		0.0169
0.054	42.1	0.00000005300474	=10.2*A60	=\$B\$1*\$D\$1*C60	
0.056	42.1	0.00000003574341	=10.2*A61	=\$B\$1*\$D\$1*C61	
0.058	42.1	0.00000002374749	=10.2*A62	=\$B\$1*\$D\$1*C62	
0.06	42.1	0.00000001554309	=10.2*A63	=\$B\$1*\$D\$1*C63	
0.065	42.1	0.000000005041761	=10.2*A64	=\$B\$1*\$D\$1*C64	
			0.679		0.0000775
0.07	42.1	0.00000000148554	=10.2*A66	=\$B\$1*\$D\$1*C66	
0.08	42.1	0.0000000001053218	=10.2*A67	=\$B\$1*\$D\$1*C67	
			0.826		0.000041
0.09	42.1	0.000000000005037118	=10.2*A69	=\$B\$1*\$D\$1*C69	
0.1	42.1	0.0000000000001683228	=10.2*A70	=\$B\$1*\$D\$1*C70	
			1.088		0.0000394
			1.487		0.0000386
0.15	42.1	3.228899E-23	=10.2*A73	=\$B\$1*\$D\$1*C73	
0.2	42.1	7.884676E-37	=10.2*A74	=\$B\$1*\$D\$1*C74	

Pu-241 Calculated vs. Observed for R=1,000,000

R =	Theta =	Total Pu			
1000000.0	0.21	Concentration			
Length (z/L)	Pore Volumes	Dissolved Pu Concentration (μCi/mL)	Depth Z (cm)	Calculated (μCi/mL)	Observed
0.001	42.1	3.72E-06	0.010	7.82E-01	
0.002	42.1	3.61E-06	0.020	7.58E-01	
0.003	42.1	3.42E-06	0.031	7.17E-01	
			0.037		1.95E-00
0.004	42.1	3.16E-06	0.041	6.64E-01	
0.005	42.1	2.86E-06	0.051	6.01E-01	
0.006	42.1	2.53E-06	0.061	5.32E-01	
0.007	42.1	2.19E-06	0.071	4.61E-01	
0.008	42.1	1.86E-06	0.082	3.90E-01	
0.009	42.1	1.54E-06	0.092	3.23E-01	
0.010	42.1	1.24E-06	0.102	2.61E-01	
0.011	42.1	9.83E-07	0.112	2.06E-01	
0.012	42.1	7.60E-07	0.122	1.60E-01	
0.013	42.1	5.75E-07	0.133	1.21E-01	
0.014	42.1	4.26E-07	0.143	8.94E-02	
0.015	42.1	3.08E-07	0.153	6.47E-02	
			0.159		4.00E-01
0.016	42.1	2.18E-07	0.163	4.57E-02	
0.017	42.1	1.51E-07	0.173	3.16E-02	
0.018	42.1	1.02E-07	0.184	2.14E-02	
0.019	42.1	6.73E-08	0.194	1.41E-02	
0.020	42.1	4.35E-08	0.204	9.13E-03	
0.021	42.1	2.74E-08	0.214	5.76E-03	
0.022	42.1	1.69E-08	0.224	3.55E-03	
0.023	42.1	1.02E-08	0.235	2.14E-03	
0.024	42.1	5.97E-09	0.245	1.25E-03	
0.025	42.1	3.41E-09	0.255	7.17E-04	
0.026	42.1	1.90E-09	0.265	4.00E-04	
0.027	42.1	1.04E-09	0.275	2.17E-04	
0.028	42.1	5.47E-10	0.286	1.15E-04	
0.029	42.1	3.14E-10	0.296	6.59E-05	
0.030	42.1	1.62E-10	0.306	3.40E-05	
0.031	42.1	8.18E-11	0.316	1.72E-05	
0.032	42.1	4.04E-11	0.326	8.48E-06	
0.033	42.1	1.95E-11	0.337	4.10E-06	
0.034	42.1	9.21E-12	0.347	1.93E-06	
			0.351		1.02E-02
0.035	42.1	4.25E-12	0.357	8.93E-07	
0.036	42.1	1.92E-12	0.367	4.03E-07	
0.037	42.1	8.47E-13	0.377	1.78E-07	
0.038	42.1	3.66E-13	0.388	7.68E-08	
0.039	42.1	1.54E-13	0.398	3.24E-08	
0.040	42.1	6.37E-14	0.408	1.34E-08	
0.041	42.1	2.57E-14	0.418	5.40E-09	
0.042	42.1	1.02E-14	0.428	2.13E-09	
0.043	42.1	3.92E-15	0.439	8.23E-10	
0.044	42.1	1.48E-15	0.449	3.11E-10	
0.045	42.1	5.46E-16	0.459	1.15E-10	
0.046	42.1	1.97E-16	0.469	4.14E-11	
0.047	42.1	6.95E-17	0.479	1.46E-11	
0.048	42.1	2.40E-17	0.490	5.04E-12	

Pu-241 Calculated vs. Observed for R=1,000,000

0.049	42.1	8.09E-18		0.500	1.70E-12	
0.050	42.1	2.67E-18		0.510	5.61E-13	
0.052	42.1	2.72E-19		0.530	5.70E-14	
				0.531		1.69E-02
0.054	42.1	2.53E-20		0.551	5.31E-15	
0.056	42.1	2.15E-21		0.571	4.51E-16	
0.058	42.1	1.67E-22		0.592	3.51E-17	
0.060	42.1	1.19E-23		0.612	2.49E-18	
0.065	42.1	1.08E-26		0.663	2.27E-21	
				0.679		7.75E-05
0.070	42.1	5.61E-30		0.714	1.18E-24	
0.080	42.1	2.82E-37		0.816	5.92E-32	
				0.826		4.10E-05
0.090	42.1	1.50E-45		0.918	3.16E-40	
0.100	42.1	6.02E-52		1.020	1.27E-46	
				1.088		3.94E-05
				1.487		3.86E-05
0.150	42.1	1.41E-11	2	1.530	2.96E-06	
0.200	42.1	1.33E-19	7	2.040	2.78E-14	



Pu-241 Calculated vs Observed for R = 1,000,000

R =	1000000	Theta = 0.21		Total Pu	
Length	Pore	Dissolved Pu		Concentration	
(z/L)	Volumes	Concentration	Depth Z (cm)	($\mu\text{Ci/mL}$)	Observed
		($\mu\text{Ci/mL}$)		Calculated	
0.001	42.1	0.00000372475	=10.2*A5	=B\$1*\$D\$1*C5	
0.002	42.1	0.000003607561	=10.2*A6	=B\$1*\$D\$1*C6	
0.003	42.1	0.000003416109	=10.2*A7	=B\$1*\$D\$1*C7	
			0.037		1.95
0.004	42.1	0.000003162857	=10.2*A9	=B\$1*\$D\$1*C9	
0.005	42.1	0.00000286334	=10.2*A10	=B\$1*\$D\$1*C10	
0.006	42.1	0.000002534592	=10.2*A11	=B\$1*\$D\$1*C11	
0.007	42.1	0.000002193681	=10.2*A12	=B\$1*\$D\$1*C12	
0.008	42.1	0.000001856362	=10.2*A13	=B\$1*\$D\$1*C13	
0.009	42.1	0.00000153596	=10.2*A14	=B\$1*\$D\$1*C14	
0.01	42.1	0.000001242625	=10.2*A15	=B\$1*\$D\$1*C15	
0.011	42.1	0.0000009830223	=10.2*A16	=B\$1*\$D\$1*C16	
0.012	42.1	0.0000007604526	=10.2*A17	=B\$1*\$D\$1*C17	
0.013	42.1	0.000000575285	=10.2*A18	=B\$1*\$D\$1*C18	
0.014	42.1	0.000000425601	=10.2*A19	=B\$1*\$D\$1*C19	
0.015	42.1	0.0000003079094	=10.2*A20	=B\$1*\$D\$1*C20	
			0.159		0.4
0.016	42.1	0.0000002178303	=10.2*A22	=B\$1*\$D\$1*C22	
0.017	42.1	0.0000001506757	=10.2*A23	=B\$1*\$D\$1*C23	
0.018	42.1	0.00000010189	=10.2*A24	=B\$1*\$D\$1*C24	
0.019	42.1	0.0000000673435	=10.2*A25	=B\$1*\$D\$1*C25	
0.02	42.1	0.0000000434938	=10.2*A26	=B\$1*\$D\$1*C26	
0.021	42.1	0.00000002744086	=10.2*A27	=B\$1*\$D\$1*C27	
0.022	42.1	0.00000001690664	=10.2*A28	=B\$1*\$D\$1*C28	
0.023	42.1	0.00000001016803	=10.2*A29	=B\$1*\$D\$1*C29	
0.024	42.1	0.00000000596684	=10.2*A30	=B\$1*\$D\$1*C30	
0.025	42.1	0.000000003414801	=10.2*A31	=B\$1*\$D\$1*C31	
0.026	42.1	0.000000001904836	=10.2*A32	=B\$1*\$D\$1*C32	
0.027	42.1	0.000000001035012	=10.2*A33	=B\$1*\$D\$1*C33	
0.028	42.1	0.0000000005474076	=10.2*A34	=B\$1*\$D\$1*C34	
0.029	42.1	0.0000000003140107	=10.2*A35	=B\$1*\$D\$1*C35	
0.03	42.1	0.0000000001620821	=10.2*A36	=B\$1*\$D\$1*C36	
0.031	42.1	0.00000000008182148	=10.2*A37	=B\$1*\$D\$1*C37	
0.032	42.1	0.00000000004039453	=10.2*A38	=B\$1*\$D\$1*C38	
0.033	42.1	0.00000000001950233	=10.2*A39	=B\$1*\$D\$1*C39	
0.034	42.1	0.000000000009207643	=10.2*A40	=B\$1*\$D\$1*C40	
			0.351		0.0102
0.035	42.1	0.000000000004251092	=10.2*A42	=B\$1*\$D\$1*C42	
0.036	42.1	0.000000000001919271	=10.2*A43	=B\$1*\$D\$1*C43	
0.037	42.1	0.0000000000008473276	=10.2*A44	=B\$1*\$D\$1*C44	
0.038	42.1	0.0000000000003657985	=10.2*A45	=B\$1*\$D\$1*C45	
0.039	42.1	0.0000000000001544206	=10.2*A46	=B\$1*\$D\$1*C46	
0.04	42.1	0.000000000000063744	=10.2*A47	=B\$1*\$D\$1*C47	
0.041	42.1	2.573014E-14	=10.2*A48	=B\$1*\$D\$1*C48	
0.042	42.1	1.015577E-14	=10.2*A49	=B\$1*\$D\$1*C49	
0.043	42.1	3.919671E-15	=10.2*A50	=B\$1*\$D\$1*C50	
0.044	42.1	1.479287E-15	=10.2*A51	=B\$1*\$D\$1*C51	
0.045	42.1	5.459088E-16	=10.2*A52	=B\$1*\$D\$1*C52	

Pu-241 Calculated vs Observed for R = 1,000,000

0.046	42.1	1.969937E-16		=10.2*A53	=\$B\$1*\$D\$1*C53	
0.047	42.1	6.951022E-17		=10.2*A54	=\$B\$1*\$D\$1*C54	
0.048	42.1	2.398329E-17		=10.2*A55	=\$B\$1*\$D\$1*C55	
0.049	42.1	8.091561E-18		=10.2*A56	=\$B\$1*\$D\$1*C56	
0.05	42.1	2.669434E-18		=10.2*A57	=\$B\$1*\$D\$1*C57	
0.052	42.1	2.716325E-19		=10.2*A58	=\$B\$1*\$D\$1*C58	
				0.531		0.0169
0.054	42.1	2.526943E-20		=10.2*A60	=\$B\$1*\$D\$1*C60	
0.056	42.1	2.149115E-21		=10.2*A61	=\$B\$1*\$D\$1*C61	
0.058	42.1	1.67099E-22		=10.2*A62	=\$B\$1*\$D\$1*C62	
0.06	42.1	1.187784E-23		=10.2*A63	=\$B\$1*\$D\$1*C63	
0.065	42.1	1.080779E-26		=10.2*A64	=\$B\$1*\$D\$1*C64	
				0.679		0.0000775
0.07	42.1	5.614259E-30		=10.2*A66	=\$B\$1*\$D\$1*C66	
0.08	42.1	2.818847E-37		=10.2*A67	=\$B\$1*\$D\$1*C67	
				0.826		0.000041
0.09	42.1	1.503412E-45		=10.2*A69	=\$B\$1*\$D\$1*C69	
0.1	42.1	6.024688E-52		=10.2*A70	=\$B\$1*\$D\$1*C70	
				1.088		0.0000394
				1.487		0.0000386
0.15	42.1	0.00000000001409654	2	=10.2*A73	=\$B\$1*\$D\$1*C73	
0.2	42.1	1.325962E-19	7	=10.2*A74	=\$B\$1*\$D\$1*C74	

APPENDIX J

**MEMORANDUM FROM
LOS ALAMOS NATIONAL LABORATORY
CHEMICAL SCIENCE AND TECHNOLOGY DIVISION**

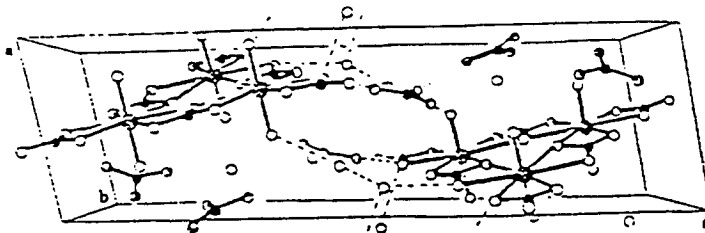
Discussion of analytical and oxidation state characterization on the 241 Actinide samples

By David L. Clark

David L. Clark
Chemical Science and Technology Division
Mail Stop G739

Los Alamos

Los Alamos National Laboratory
Los Alamos, New Mexico 87545



Dan,

Here is a discussion of the analytical and oxidation state characterization on the ^{241}Am Actinide samples.

(1) ^{241}Am (III) preparation and characterization.

LANL CST-7 prepared a sample of aqueous $^{241}\text{Am}^{3+}$ for assay and shipment to Sandia National Laboratory. Preparation and assay are recorded in LANL lab notebook LA-CST-NBK-95-028, pages 35-36, and 38-39. The results of the ^{241}Am assay are recorded on page 41. Approximately 0.025g of high purity $^{241}\text{AmO}_2$ (lot ID LRA03) was taken from Material Balance Area 528 and dissolved in 0.5mL 8M HNO_3 with a trace amount of HF. This solution was heated in a salt bath until the solid had dissolved to give a yellow solution. The ^{241}Am was precipitated from solution using 10.7M NaOH. The resulting $^{241}\text{Am}(\text{OH})_3$ was removed via centrifugation, and washed three times with distilled water. The resulting precipitate was redissolved in 0.5mL of 1M HClO_4 to give a pink solution of $^{241}\text{Am}^{3+}$ aquo ion. An 0.025mL aliquot of this solution was added to 3.0 mL of 1M HClO_4 and added to a 2cm micro cell for assay using absorption spectroscopy. The absorption maximum at 503 nm was used to determine Am concentration, and to confirm that all Am was present in the trivalent oxidation state. Another aliquot was submitted for isotopic purity determination (Analytical Chemistry sample ID 200017115). Alpha spectroscopy showed only ^{241}Am , and total plutonium < 0.6% of alpha activity. The combined assays were used to prepare 5.0 mL of a solution containing $1.03 \times 10^{-6}\text{M}$ $^{241}\text{Am}^{3+}$ in 0.1M HCl. This solution was packaged and shipped to Dan Lucero at SNL.

(2) ^{241}Pu sample analysis.

LANL CST-7 received a shipment of ^{241}Pu from Dan Lucero at SNL. This sample contained 19.91 $\mu\text{Ci/g}$ of ^{241}Pu in 1M HCl as of December 1, 1994. A simple calculation suggested that 19.60 $\mu\text{Ci/g}$ of ^{241}Pu in 1M HCl existed as of April 1, 1995. This activity corresponded to a concentration of $7.2 \times 10^{-7}\text{M}$, which is at the edge of our detection limits for oxidation state determination using PAS. Since this was the only ^{241}Pu available, the risk of losing sample via transfers, etc. was deemed too great, and we sent the sample back to SNL. The status of the oxidation state of the sample is unclear. Normally, in HCl solution, alpha radiolysis will keep the sample in the tetravalent oxidation state. However, ^{241}Pu is primarily a beta-emitting radionuclide, and the radiolysis effects from such a solution are not well understood. Plutonium samples in near-neutral solution under these concentrations are known to contain a large amount of the pentavalent oxidation state. Without further data in brine solution, one cannot say for sure what the predominant oxidation state will be.



Dr. David L. Clark
Chemical Science and Technology Division
Mail Stop G739

Phone: (505) 665-4622
FAX: (505) 665-4624
e-mail: DLCLARK@LANL.GOV